Table 1. Maps relevant to genes for which the expression was affected in the liver of ConA-injected mice followed by ADSC treatment at 3 h.

Maps	*p*-value
Tissue remodeling and wound repair	0.000001438
Inflammatory response	0.000003973
Mitogenic signaling	0.0001056
Vascular development (angiogenesis)	0.0002926
DNA damage response	0.0004529
Apoptosis	0.0008909
Cystic fibrosis disease	0.001402
Myogenesis regulation	0.001571
Cell differentiation	0.002173
Immune system response	0.003304

In conclusion, the therapeutic anti-inflammatory efficacy of ADSCs relied on suppression of myeloid-lineage and $CD4^+$ T cells in the ConA-induced C57BL/6 murine hepatitis model. The application of ADSC therapy to various inflammatory liver diseases can be further developed by studies of their immunomodulatory effects.

Materials and methods

Murine acute hepatitis induced by ConA injection and treatment with ADSCs

C57BL/6J female mice (10–12 weeks old, Charles River Laboratories Japan Inc., Yokohama, Japan) were injected i.v. with 300 μg of ConA (Sigma-Aldrich, St. Louis, MO, USA) dissolved in PBS. For $CD4^+$ T-cell or $CD8^+$ T-cell depletion, 200 μg of purified anti-CD4 antibody from the culture supernatant of GK1.5 cells (ATCC, Manassas, VA, USA), or purified anti-CD8 antibody from the culture supernatant of 2.43 cells (ATCC), was injected i.p. for two consecutive days before ConA injection. For depletion of monocyte-macrophage lineage cells, 2 mg of clodronate (Sigma-Aldrich), which was encapsulated in liposomes using the COATSOME-EL-01-N liposome formulation kit (Nihonyushi, Tokyo, Japan) [27], was injected via the tail vein 2 days before ConA injection. For the prevention or treatment experiment, 1×10^5 ADSCs were administered i.v. immediately or 3 h after ConA injection. In some cohorts, blood was obtained under anesthesia, and liver and lung tissues were collected after euthanizing mice at 6, 12, and 24 h after ConA injection. A portion of the liver tissue was homogenized and the enriched fraction of inflammatory cells was obtained by gradient centrifugation using Ficoll–Hypaque (Sigma-Aldrich). Our institutional review board approved the care and use of laboratory animals in all experiments.

Isolation and culture of ADSCs and primary hepatocytes

Inguinal adipose tissues were obtained from C57BL/6J male mice (10–12 weeks old, Charles River Laboratories Japan Inc.) or GFP-transgenic mice (male, 10–12 weeks old, gift from Prof. Okabe, Osaka University, Japan). Tissues were digested with 0.075% collagenase type I (Wako Pure Chemical Industries Ltd., Osaka, Japan), washed with PBS, and then transferred to a culture dish with DMEM/F-12 1:1 medium (Life Technologies–Invitrogen, Carlsbad, CA, USA) supplemented with 10% heat-inactivated FBS and 1% antibiotic–antimycotic solution (Life Technologies). Cells were maintained and expanded by eight to ten passages before use.

To obtain primary hepatocytes, C57BL/6J male mice (10–12 weeks old) were anesthetized by i.p. injection of pentobarbital (50 mg/kg; Kyoritsu Seiyaku, Tokyo, Japan) and injected with 10 mL of 0.75% type I collagenase solution via the portal vein. Liver tissues were minced to dissociate cells, filtered through a 100 μm mesh, and cultured in 10-cm culture dishes for 16 h until use.

Pluripotency of ADSCs

The pluripotency of ADSCs was examined using a mouse mesenchymal stem cell functional kit® (R&D Systems, Minneapolis, MN, USA), and immunohistochemical staining of cells that had differentiated into osteocytes, chondrocytes, and adipocytes was performed using anti-mouse ostepontin, anti-mouse collagen II, and anti-mouse FABP4 antibodies, respectively, in accordance with the manufacturer's instruction. Adipocyte differentiation was also assessed by staining using an aliquot of Oil Red O (WAKO).

Co-culture of ConA-stimulated hepatic inflammatory cells with ADSCs

Hepatic inflammatory cells were isolated from C57BL/6J female mice (10 weeks old) that had been injected i.v. with 300 μg of ConA 3 h before ($n = 4$). $CD4^+$ T cells and $CD11b^+$ cells were separated from the collected hepatic inflammatory cells using anti-CD4 and anti-CD11b magnetic beads (Miltenyi Biotec, Bergisch Gladbach, Germany). Then, 20 000 ADSCs were co-cultured with 4×10^5 of the isolated $CD4^+$ T cells or $CD11b^+$ cells in a 24-well plate (BD Falcon, San Jose, CA, USA) for 2 h ($n = 3$). After co-culture, floating cells were harvested, and RNA harvested using the MicroRNA isolation kit (Stratagene, La Jolla, CA, USA) for real-time PCR analysis to measure cytokine/chemokine gene expression.

Measurement of serum ALT and LDH activity

Blood was collected from the postorbital venous plexus and serum was separated from clotted blood after coagulation. The serum activity of ALT, and LDH was measured using L-type WAKO GPT J2, and LDH-J kits (Wako Pure Chemical Industries Ltd.), respectively, using autoanalytical equipment (Hitach7180, Hitachi Ltd., Tokyo, Japan), according to the manufacturer's protocol.

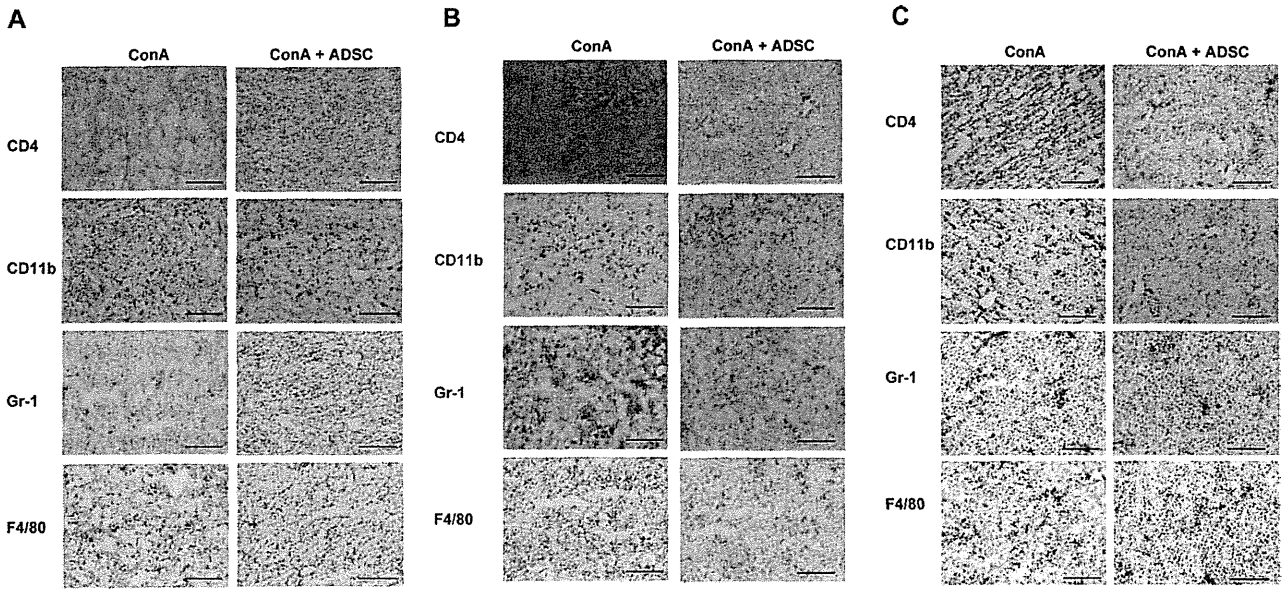

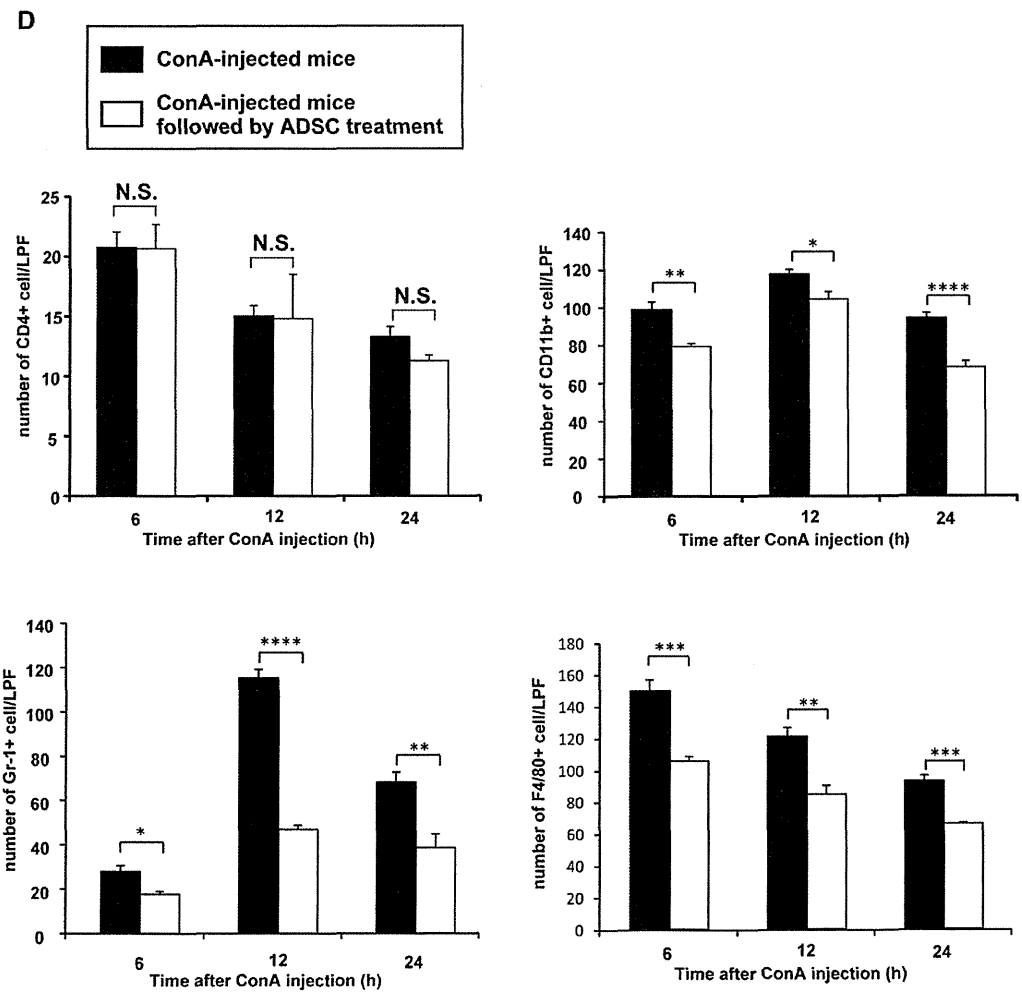

Measurement of serum cytokine/chemokine concentrations

Sera were obtained from ADSC-treated mice immediately or 3 h after ConA injection ($n = 3$ and $n = 4$, respectively), and from ConA-injected mice not treated with ADSCs ($n = 3$ and $n = 6$, respectively) at 6 h. Serum concentrations of cytokines and chemokines were measured using a Multiplex Bead Immunoassays kit, Mouse Cytokine 20-Plex Panel (Invitrogen, Carlsbad, CA, USA), following the manufacturer's protocol. The kit covers FGF-basic, GM-CSF, IFN-γ, IL-1α, IL-1β, IL-2, IL-4, IL-5, IL-6, IL-10, IL-12 (p40/p70), IL-13, IL-17, IP-10(CXCL10), KC, MCP-1, MIG(CXCL9), MIP-1α, TNF-α, and VEGF.

Histological and immunohistochemical analyses of liver and lung tissues

Harvested liver and lung tissues were fixed in 10% formaldehyde, embedded in paraffin, sectioned at 4 μm, and stained with H&E. For immunohistochemical analysis, the liver tissues were embedded in OCT compound (Sakura Finetek, Torrance, CA, USA), snap-frozen in liquid nitrogen, cryostat-sectioned, and fixed with methanol/acetone (1:1). The paraffin-embedded tissues were also sliced into 4 μm sections, mounted on microscope slides, and deparaffinized, followed by epitope retrieval using proteinase K (Dako, Glostrup, Denmark). The slides were incubated with peroxidase blocking reagent (Dako) for 15 min at room temperature to inhibit endogenous peroxidase activity, followed by incubation with protein blocking reagent (Dako) to avoid nonspecific protein reactions. The slides were incubated with primary antibodies (anti-mouse CD4, CD11b, Gr-1, F4/80) (BD Pharmingen, San Diego, CA, USA) and anti-GFP (MBL, Nagoya, Japan) diluted with PBS containing 1% BSA overnight at 4°C. After washing in PBS, the slides were then incubated with secondary antibodies (anti-rat, anti-rabbit; Nichirei, Japan) for 30 min at room temperature. The immune complexes were visualized using EnVision kits /HRP (DAB; Dako) followed by counterstaining with hematoxylin. The numbers of positive cells in each section were counted in four randomly selected fields at 100× magnification under a microscope.

RNA isolation and gene expression analysis by DNA microarray

Total RNA was obtained from the tissues or hepatic inflammatory cells in RNAlater (Ambion) using RNA isolation kit (Sigma-Aldrich) in accordance with the supplied protocol with slight modifications. Isolated RNA was amplified and labeled with the Cy3 using the Quick Amp labeling kit (Agilent Technologies, Santa Clara, CA, USA) in accordance with the manufacturer's protocol. cRNA of 1.65 μg was hybridized onto a Whole Mouse Genome 4 × 44K Array (Agilent Technologies) and scanned using a DNA Microarray Scanner (model G2505B, Agilent Technologies).

Gene expression data were analyzed using the GeneSpring analysis software (Agilent Technologies). Each measurement was divided by the 75th percentile of all measurements in that sample at per chip normalization. Hierarchical clustering and principal component analysis of gene expression was performed. Welch's *t*-test, with Benjamini and Hochberg's false discovery rate, was used to identify genes that were differentially expressed in the groups of interest. Analysis of biological processes was performed using the MetaCore software suite (GeneGo, Carlsbad, CA, USA). BRB array tools (http://linus.nci.nih.gov/BRB-ArrayTools.html) were also used for unsupervised or one-way clustering analyses. Microarray data were deposited in the NBCI Gene Expression Omnibus (GSE ID: GSE41465).

Flow cytometry

Cultured ADSCs were incubated in PBS supplemented with 2% BSA (Sigma-Aldrich) containing antibodies labeled with FITC or PE anti-mouse CD44 or CD90 (Beckman Coulter, Brea, CA, USA), and CD105 (Miltenyi Biotec) antibodies. Hepatic inflammatory cells isolated from mice were incubated with a mixture of FITC-labeled anti-mouse CD204 (AbD Serotec, Raleigh, NC, USA), PE-labeled anti-mouse Gr-1 (Miltenyi Biotec), and allophycocyanin-labeled anti-mouse CD11b (BioLegend, San Diego, CA, USA), or FITC-labeled anti-mouse CD11b (Beckman Coulter), PE-labeled anti-mouse Ly-6G (BioLegend), and allophycocyanin labeled anti-mouse Ly-6C (BioLegend) antibodies. The fluorescence intensity of the cells was measured using a FACSCalibur™ (Becton Dickinson, San Jose, CA, USA). Data obtained were visualized and analyzed using the FlowJo software (Tomy Digital Biology Co., Ltd., Tokyo, Japan).

Isolation of $CD11b^+Gr\text{-}1^+$ hepatic inflammatory cells and T-cell [3H]-thymidine incorporation assay

C57BL/6J female mice were injected with 300 μg of ConA and then injected with 1×10^5 ADSCs after 3 h ($n = 3$). Three

Figure 5. Immunohistochemical analysis of inflammatory cells in the liver of ConA-induced hepatitis mice treated with ADSCs. (A–C) Immunohistochemical staining of the liver. C57BL/6 female mice were injected i.v. with 300 μg of ConA. Then, 3 h later, the mice were injected with ADSCs via the tail vein. Liver tissues were obtained at (A) 6, (B)12, or (C) 24 h after ConA injection ($n = 4$ per each time point). Immunohistochemical staining was conducted using anti-CD4, anti-CD11b, anti-Gr-1, and anti-F4/80 antibodies. Stained liver images shown are representative of three experiments performed. Magnification: ×100. Bars: 200 μm. (D) Quantification of $CD4^+$, $CD11b^+$, $Gr\text{-}1^+$, and $F4/80^+$ cells in four visual fields per ×100 low-power field in the liver of representative mice from each group. Data are shown as mean +SE ($n = 4$) and are representative of three experiments performed. $^*p < 0.05$, $^{**}p < 0.01$, $^{***}p < 0.005$, $^{****}p < 0.001$; Student's *t*-test. n.s.: not significant.

hours later, hepatic inflammatory cells were isolated and incubated with FITC-labeled anti-mouse CD11b (Beckman Coulter) and PE-labeled anti-mouse Gr-1 (Miltenyi Biotec) antibodies. The $CD11b^+Gr\text{-}1^+$ population was collected using a FACSAira II™ (Becton Dickinson). $CD11b^+Gr\text{-}1^+$ cells (1×10^5), which had been irradiated with 2000 rads, were co-cultured with 1×10^5 purified splenic T cells isolated from C57BL/6J mice in RPMI1640 medium (Invitrogen) supplemented with 10% heat-inactivated FBS, 1% antibiotic–antimycotic solution (Life Technologies), and ConA (4 μg/mL) for 48 h ($n = 4$). The culture was pulsed with [3H]thymidine (1 μCi/well) for 16 h and harvested. Thymidine incorporation was measured using a beta-counter (PerkinElmer, Waltham, MA, USA).

NO assay

C57BL/6J female mice were injected with 300 μg of ConA. Three hours later, 1×10^5 ADSCs were injected via the tail vein. After a further 3 h, hepatic inflammatory cells were isolated from ConA hepatitis mice with or without ADSC treatment ($n = 3$ each) and incubated in PBS supplemented with 2% BSA, PE-labeled anti-mouse Gr-1 antibody, and allophycocyanin-labeled anti-mouse CD11b antibody. Cells were then incubated in PBS containing 2.5 mg/mL diaminofluorescein-FM diacetate (Sekisui Medical Co., Ltd., Tokyo, Japan), which emits fluorescence at 515 nm in a reaction with NO, at 37°C for 30 min and subjected to FACS analysis using a FACSCalibur flow cytometer.

Arginase assay

Female C57BL/6J mice were injected with 300 μg of ConA. Three hours later, 1×10^5 ADSCs were injected via the tail vein. After further 3 h, hepatic inflammatory cells were isolated from ConA hepatitis mice with or without ADSC treatment ($n = 3$ each) and were lysed with PBS containing 10 mM Tris-HCl (pH 7.4) and 0.4% Triton X-100, supplemented with the proteinase inhibitor cocktail, cOmplete, Mini, EDTA-free® (Roche, Basel, Switzerland). One hundred micrograms of the lysis aliquot obtained were subject to an arginase activity assay using a QuantiChrom™ Arginase Assay kit (BioAssay Systems, Hayward, CA), which measures urea produced from the substrate, in accordance with the manufacturer's protocol.

Statistical analysis

All data are expressed as means ± SE. Statistical analyses were performed using the JMP software (ver.9.02; SAS Institute Japan Inc., Tokyo, Japan). Student's *t*-test and Wilcoxon signed-rank test were used. p values < 0.05 were considered to indicate statistical significance.

Acknowledgements: This study was supported, in part, by subsidies from the Japanese Ministry of Education, Culture, Sports, Science, and Technology and the Japanese Ministry of Health, Labor, and Welfare.

Conflict of interest: The authors declare no financial or commercial conflict of interest.

References

1 Zuk, P. A., Zhu, M., Ashjian, P., De Ugarte, D. A., Huang, J. I., Mizuno, H., Alfonso, Z. C. et al., Human adipose tissue is a source of multipotent stem cells. *Mol. Biol. Cell* 2002. **13**: 4279–4295.

2 Chamberlain, G., Fox, J., Ashton, B. and Middleton, J., Concise review: mesenchymal stem cells: their phenotype, differentiation capacity, immunological features, and potential for homing. *Stem Cells* 2007. **25**: 2739–2749.

3 Perez-Cano, R., Vranckx, J. J., Lasso, J. M., Calabrese, C., Merck, B., Milstein, A. M., Sassoon, E. et al., Prospective trial of adipose-derived regenerative cell (ADRC)-enriched fat grafting for partial mastectomy defects: the RESTORE-2 trial. *Eur. J. Surg. Oncol.* 2012. **38**: 382–389.

4 Janssens, S., Stem cells in the treatment of heart disease. *Annu. Rev. Med.* 2010. **61**: 287–300.

5 Hoogduijn, M. J., Popp, F., Verbeek, R., Masoodi, M., Nicolaou, A., Baan, C. and Dahlke, M. H., The immunomodulatory properties of mesenchymal stem cells and their use for immunotherapy. *Int. Immunopharmacol.* 2010. **10**: 1496–1500.

6 Baroni, G. S., Pastorelli, A., Manzin, A., Benedetti, A., Marucci, L., Solforosi, L., Di Sario, A. et al., Hepatic stellate cell activation and liver fibrosis are associated with necroinflammatory injury and Th1-like response in chronic hepatitis C. *Liver* 1999. **19**: 212–219.

7 Cerny, A. and Chisari, F. V., Pathogenesis of chronic hepatitis C: immunological features of hepatic injury and viral persistence. *Hepatology* 1999. **30**: 595–601.

8 Gershwin, M. E., Ansari, A. A., Mackay, I. R., Nakanuma, Y., Nishio, A., Rowley, M. J. and Coppel, R. L., Primary biliary cirrhosis: an orchestrated immune response against epithelial cells. *Immunol. Rev.* 2000. **174**: 210–225.

9 Krawitt, E. L., Autoimmune hepatitis. *N. Engl. J. Med.* 1996. **334**: 897–903.

10 Fujii, H. and Kawada, N., Inflammation and fibrogenesis in steatohepatitis. *J. Gastroenterol.* 2012. **47**: 215–225.

11 Dienes, H. P. and Drebber, U., Pathology of immune-mediated liver injury. *Dig. Dis.* 2010. **28**: 57–62.

12 Dai, L. J., Li, H. Y., Guan, L. X., Ritchie, G. and Zhou, J. X., The therapeutic potential of bone marrow-derived mesenchymal stem cells on hepatic cirrhosis. *Stem Cell Res.* 2009. **2**: 16–25.

13 Sanders, D. A., Moothoo, D. N., Raftery, J., Howard, A. J., Helliwell, J. R. and Naismith, J. H., The 1.2 A resolution structure of the Con A-dimannose complex. *J. Mol. Biol.* 2001. **310**: 875–884.

14 Kato, M., Ikeda, N., Matsushita, E., Kaneko, S. and Kobayashi, K., Involvement of IL-10, an anti-inflammatory cytokine in murine liver injury induced by concanavalin A. *Hepatol. Res.* 2001. **20**: 232–243.

15 **Kubo, N., Narumi, S., Kijima, H., Mizukami, H., Yagihashi, S., Hakamada, K. and Nakane, A.**, Efficacy of adipose tissue-derived mesenchymal stem cells for fulminant hepatitis in mice induced by concanavalin A. *J. Gastroenterol. Hepatol.* 2012. **27**: 165–172.

16 **Murdoch, C., Muthana, M., Coffelt, S. B. and Lewis, C. E.**, The role of myeloid cells in the promotion of tumour angiogenesis. *Nat. Rev. Cancer* 2008. **8**: 618–631.

17 **Banas, A., Teratani, T., Yamamoto, Y., Tokuhara, M., Takeshita, F., Quinn, G., Okochi, H. et al.**, Adipose tissue-derived mesenchymal stem cells as a source of human hepatocytes. *Hepatology* 2007. **46**: 219–228.

18 **Kaneko, Y., Harada, M., Kawano, T., Yamashita, M., Shibata, Y., Gejyo, F., Nakayama, T. et al.**, Augmentation of Valpha14 NKT cell-mediated cytotoxicity by interleukin 4 in an autocrine mechanism resulting in the development of concanavalin A-induced hepatitis. *J. Exp. Med.* 2000. **191**: 105–114.

19 **Tiegs, G., Hentschel, J. and Wendel, A.**, A T cell-dependent experimental liver injury in mice inducible by concanavalin A. *J. Clin. Invest.* 1992. **90**: 196–203.

20 **Halder, R. C., Aguilera, C., Maricic, I. and Kumar, V.**, Type II NKT cell-mediated anergy induction in type I NKT cells prevents inflammatory liver disease. *J. Clin. Invest.* 2007. **117**: 2302–2312.

21 **Schwabe, R. F. and Brenner, D. A.**, Mechanisms of liver injury. I. TNF-alpha-induced liver injury: role of IKK, JNK, and ROS pathways. *Am. J. Physiol. Gastrointest. Liver Physiol.* 2006. **290**: G583–G589.

22 **Schumann, J., Wolf, D., Pahl, A., Brune, K., Papadopoulos, T., van Rooijen, N. and Tiegs, G.**, Importance of Kupffer cells for T-cell-dependent liver injury in mice. *Am. J. Pathol.* 2000. **157**: 1671–1683.

23 **Clegg, C. H., Rulffes, J. T., Wallace, P. M. and Haugen, H. S.**, Regulation of an extrathymic T-cell development pathway by oncostatin M. *Nature* 1996. **384**: 261–263.

24 **Constant, S. L. and Bottomly, K.**, Induction of Th1 and Th2 CD4+ T cell responses: the alternative approaches. *Annu. Rev. Immunol.* 1997. **15**: 297–322.

25 **Contento, R. L., Molon, B., Boularan, C., Pozzan, T., Manes, S., Marullo, S. and Viola, A.**, CXCR4-CCR5: a couple modulating T cell functions. *Proc. Natl. Acad. Sci. USA* 2008. **105**: 10101–10106.

26 **Ponte, A. L., Marais, E., Gallay, N., Langonne, A., Delorme, B., Herault, O., Charbord, P. et al.**, The in vitro migration capacity of human bone marrow mesenchymal stem cells: comparison of chemokine and growth factor chemotactic activities. *Stem Cells* 2007. **25**: 1737–1745.

27 **Kushiyama, T., Oda, T., Yamada, M., Higashi, K., Yamamoto, K., Oshima, N., Sakurai, Y. et al.**, Effects of liposome-encapsulated clodronate on chlorhexidine gluconate-induced peritoneal fibrosis in rats. *Nephrol. Dial. Transplant.* 2011. **26**: 3143–3154.

Abbreviations: **ADSC**: adipose tissue derived stromal stem cell · **ALT**: alanine transferase · **LDH**: lactate dehydrogenase · **MDSC**: myeloid-derived suppressor cell · **MSC**: mesenchymal stromal stem cell

Full correspondence: Dr. Shuichi Kaneko, Disease Control and Homeostasis, Kanazawa University, 13-1 Takara-machi, Kanazawa, Ishikawa 920-8641, Japan
Fax: +81-76-234-4250
e-mail: skaneko@m-kanazwa.jp

Received: 17/3/2013
Revised: 3/7/2013
Accepted: 6/8/2013
Accepted article online: 12/8/2013

Published OnlineFirst February 20, 2013; DOI: 10.1158/1078-0432.CCR-12-1641

Clinical Cancer Research

Imaging, Diagnosis, Prognosis

Association of *Interleukin-28B* Genotype and Hepatocellular Carcinoma Recurrence in Patients with Chronic Hepatitis C

Yuji Hodo[1], Masao Honda[1,3], Akihiro Tanaka[1], Yoshimoto Nomura[1], Kuniaki Arai[1], Taro Yamashita[1], Yoshio Sakai[1], Tatsuya Yamashita[1], Eishiro Mizukoshi[1], Akito Sakai[1], Motoko Sasaki[2], Yasuni Nakanuma[2], Mitsuhiko Moriyama[4], and Shuichi Kaneko[1]

Abstract

Purpose: Several single-nucleotide polymorphisms (SNP) in the interleukin-28B (*IL-28B*) locus have recently been shown to be associated with antiviral treatment efficacy for chronic hepatitis C (CHC). However, such an association with hepatocellular carcinoma (HCC) is unkno3 we investigated the association between the *IL-28B* genotype and the biology and clinical outcome of patients with HCC receiving curative treatment.

Experimental Design: Genotyping of 183 patients with HCC with CHC who were treated with hepatic resection or radiofrequency ablation (RFA) was carried out, and the results were analyzed to determine the association between the *IL-28B* genotype (rs8099917) and clinical outcome. Gene expression profiles of 20 patients with HCC and another series of 91 patients with CHC were analyzed using microarray analysis and gene set enrichment analysis. Histologic and immunohistochemical analyses were also conducted.

Results: The TT, TG, and GG proportions of the rs8099917 genotype were 67.8% (124 of 183), 30.6% (56 of 183), and 1.6% (3 of 183), respectively. Multivariate Cox proportional hazard analysis showed that the *IL-28B* TT genotype was significantly associated with HCC recurrence ($P = 0.007$; HR, 2.674; 95% confidence interval, 1.16–2.63). Microarray analysis showed high expression levels of IFN-stimulated genes in background liver samples and immune-related genes in tumor tissues of the *IL-28B* TG/GG genotype. Histologic findings showed that more lymphocytes infiltrated into tumor tissues in the TG/GG genotype.

Conclusions: The *IL-28B* genotype is associated with HCC recurrence, gene expression, and histologic findings in patients with CHC. *Clin Cancer Res; 19(7); 1827–37. ©2013 AACR.*

Introduction

Hepatocellular carcinoma (HCC) is the seventh most common cancer worldwide and the third most common cause of cancer mortality (1). HCC usually develops in patients suffering from chronic hepatitis B or chronic hepatitis C (CHC). Although hepatic resection has been considered the most efficient therapy for HCC, it is only suitable for 20% to 35% of patients because of poor hepatic reserve (2). Radiofrequency ablation (RFA) has therefore been introduced as a minimally invasive therapy for such cirrhotic patients and is widely applicable with little effect on hepatic reserve. Moreover, randomized (3, 4) and nonrandomized (5, 6) controlled studies revealed no statistical difference in patient survival between resection and RFA.

Despite these curative treatments of HCC, its recurrence remains common. Several studies have identified potential risk factors for HCC recurrence, including the presence of cirrhosis, high α-fetoprotein (AFP) levels, large tumor foci, and tumor multiplicity (7, 8).

The interleukin-28B (*IL-28B*) gene, also known as IFN-λ3, is a newly described member of the family of IFN-related cytokines (9) and shares the same biologic properties as type I IFNs (10). Recently, several single-nucleotide polymorphisms (SNP) in the *IL-28B* locus have been associated with the effectiveness of pegylated-IFN and ribavirin combination therapy for CHC (11, 12). We previously confirmed this relationship and revealed that the *IL-28B* genotype is associated with the expression of hepatic IFN-stimulated genes (ISG) in patients with CHC (13). Others have also described an association between the *IL-28B* genotype and the outcome of CHC therapy, biochemical factors, and histologic findings (14, 15); however, the relationship between the *IL-28B* genotype and the biology and clinical course of HCC remains unknown. In this study,

Authors' Affiliations: Departments of [1]Gastroenterology and [2]Human Pathology, Kanazawa University Graduate School of Medical Science; [3]Department of Advanced Medical Technology, Kanazawa University Graduate School of Health Medicine, Kanazawa, Ishikawa; and [4]Third Department of Internal Medicine, Nihon University School of Medicine, Tokyo, Japan

Note: Supplementary data for this article are available at Clinical Cancer Research Online (http://clincancerres.aacrjournals.org/).

Corresponding Author: Shuichi Kaneko, Department of Gastroenterology, Kanazawa University Graduate School of Medical Science, 13-1 Takara-Machi, Kanazawa, Ishikawa 920-8641, Japan. Phone: 81-76-265-2235; Fax: 81-76-234-4250; E-mail: skaneko@m-kanazawa.jp

doi: 10.1158/1078-0432.CCR-12-1641

Published OnlineFirst February 20, 2013; DOI: 10.1158/1078-0432.CCR-12-1641

Translational Relevance

Several single-nucleotide polymorphisms (SNP) in the interleukin-28B (*IL-28B*) locus have recently been shown to be associated with antiviral treatment efficacy in chronic hepatitis C (CHC). In this study, we investigated the association between the *IL-28B* genotype (rs8099917) and the biology and clinical outcome of patients with hepatocellular carcinoma (HCC) receiving curative treatment. Patients with the *IL-28B* TT genotype had a significantly higher incidence of HCC recurrence than patients with the TG/GG genotype. Gene expression profile and histologic analysis showed that the immune response and chronic hepatitis inflammation were more severe in patients with the TT genotype. Conversely, the expression of IFN-stimulated genes was upregulated and the immune response to tumors was more intense in those with the TG/GG genotype. These finding suggest that such molecular mechanisms may affect HCC recurrence.

therefore, we investigated the association between the *IL-28B* genotype and clinical outcome after initial curative treatment of HCC and clarified the molecular features in relation to the *IL-28B* genotype.

Materials and Methods

Patients

A total of 852 patients were admitted to the Department of Gastroenterology, Kanazawa University Hospital, Kanazawa, Japan between January 2000 and March 2012 for the treatment of developed HCC. The major background liver disease was hepatitis C virus (HCV; $n = 502$), followed by hepatitis B virus ($n = 148$). Treatment of HCC included surgical resection in 175 patients and RFA in 390 patients. The choice of treatment procedure was determined according to the extent of the tumor and the hepatic functional reserve as assessed by Child's classification that forms the Japanese HCC Guidelines (16, 17). In some cases indicated for surgical resection, we conducted RFA on patients who refused surgical resection, and we consequently excluded these patients on the basis of Japanese HCC guidelines.

Study inclusion criteria were: (i) Child–Pugh class A or B; (ii) the presence of up to 3 tumors, each 3 cm or less; (iii) HCV infection (positive for HCV RNA, patients with sustained viral response were excluded); (iv) radical treatment by either surgical resection or RFA; and (v) availability of blood samples for genetic analyses (Supplementary Fig. S1). Consequently, 183 patients were studied and their baseline characteristics are reported in Table 1. Informed consent was obtained from all patients before therapy. The experimental protocol was approved by the Human Genome, Gene Analysis Research Ethics Committee of Kanazawa University (Approval No. 260), and the study was conducted in accordance with the Declaration of Helsinki.

Diagnosis of HCC

HCC diagnosis was based predominantly on image analysis. Patients underwent dynamic computed tomography (CT) and/or dynamic MRI and abdominal angiography with CT imaging in the arterial and portal flow phase. HCC was diagnosed if a liver nodule showed hyperattenuation in the arterial phase and washout in the portal or delayed phase or showed typical hypervascular staining on digital subtraction angiography (18).

Table 1. Clinical features of 183 patients with HCC at entry by *IL-28B* genotype

Variables	*IL-28B* TT genotype ($n = 124$)	*IL-28B* TG/GG genotype ($n = 59$)	*P*
Sex (male:female)	76:48	32:27	0.422
Age, y (≤70:>70)	64:60	32:27	0.754
Platelet count ($\times 10^4/mm^3$; ≤10:>10)	68:56	28:31	0.429
ALT, IU/L (≤40:>40)	44:80	25:34	0.416
γ-GTP, IU/L (≤50:>50)	46:78	21:38	0.871
Albumin, g/dL (≤3.5:>3.5)	41:83	12:47	0.084
Protrombin activity, % (≤70:>70)	28:96	9:50	0.325
Total bilirubin, mg/dL (≤2:>2)	7:117	1:58	0.440
Child–Pugh class (A:B)	77:29	43:10	0.352
Therapy (resection: RFA)	19:105	10:49	0.830
Period of therapy (2000-05:2006-12)	41:83	21:38	0.741
History of IFN therapy (yes:no)	56:68	26:33	0.999
Tumor number (solitary: 2–3)	80:44	42:17	0.406
Tumor size, mm (≤20:>20)	83:41	36:23	0.508
AFP, ng/mL (≤20:>20)	60:64	37:22	0.082
DCP, AU/L (≤40:>40)	75:49	39:20	0.516

Published OnlineFirst February 20, 2013; DOI: 10.1158/1078-0432.CCR-12-1641

Method of treatment

Hepatic resection was carried out under intraoperative ultrasonographic monitoring and guidance. Anatomic resection was conducted in 9 patients and nonanatomic resection was conducted in 20 patients. Curative resection was defined as removal of all recognizable tumors with a clear margin (19). RFA was conducted using either the radiofrequency interstitial tumor ablation system (RITA; RITA Medical Systems Inc.) or the cool-tip system (Tyco Healthcare Group LP). All procedures were conducted according to the manufacturer's protocol. In the case of RFA, dynamic CT was conducted 1 to 3 days after therapy and the ablated area was evaluated. Complete ablation was defined as no enhancement in the ablated area on the dynamic CT. When complete ablation was not achieved, additional ablation was considered.

Follow-up

All patients were followed up by ultrasound and contrast enhancement 3-phase CT or MRI every 3 months. Local tumor progression was defined as the reappearance of tumor progression adjacent to the treated site and distant recurrence as the emergence of one or several tumor(s) not adjacent to the treated site. Patients with confirmed recurrence received further treatment such as resection, RFA, transarterial chemoembolization, and chemotherapy depending on the condition. Time to recurrence (TTR) was defined as the period from the date of therapy until the detection of tumor recurrence, death, or the last follow-up assessment. For TTR analysis, the data were censored for patients without signs of recurrence.

Genetic variation of the *IL-28B* polymorphism

Genomic DNA was extracted from peripheral blood samples using the QIAamp DNA Blood Mini Kit (Qiagen) according to the manufacturer's instructions. An *IL-28B* SNP (rs8099917) was determined using TaqMan Pre-Designed SNP Genotyping Assays as described previously (12). A custom assay was created by Applied Biosystems for rs12979860. We determined *IL-28B* genetic variations in all patients included in this study.

Affymetrix genechip analysis

Resected cancer and noncancerous liver tissue specimens were immediately frozen in liquid nitrogen and kept at −80°C until required for RNA preparation. Liver tissue RNA was isolated using the RNeasy Mini Kit (Qiagen) according to the manufacturer's instructions. Isolated RNA was stored at −70°C until required. The quality of isolated RNA was estimated after electrophoresis using an Agilent 2001 Bioanalyzer. Microarray analysis using an Affymetrix Human 133 Plus 2.0 microarray chip was conducted as described previously (13). The microarray data have been submitted to the Gene Expression Omnibus (GEO) public database at National Center for Biotechnology Information (NCBI, Bethesda, MD; accession number GSE41804).

Gene set enrichment analysis

Affymetrix GeneChip array data were normalized, preprocessed, and analyzed using R (20) and Bioconductor (21) software. Raw CEL file data were normalized using the MAS 5.0 algorithm as implemented in the *affy* package. Normalized data were $\log_2$ transformed and assessed using gene set enrichment analysis (GSEA), which is a bioinformatics method to assess whether genes with known biological/molecular function are concomitantly upregulated or downregulated in a certain gene expression dataset (22). GSEA was conducted using a parametric analysis of gene set enrichment (PAGE; ref. 23). The Gene Ontology gene set collection C5 of the Molecular Signatures Database (22) was downloaded from the Broad Institute and loaded into the R environment.

We also investigated the gene set differentially expressed HCC-infiltrating mononuclear inflammatory cells studied previously (24). *Z* scores and *P* values of all gene sets were calculated using the *PGSEA* package and an estimate was made as to whether certain gene sets, and therefore functional gene categories, were differentially regulated in HCC tissue from patients with the *IL-28B* TT genotype and the *IL-28B* TG/GG genotype.

Hierarchical clustering

Hierarchical clustering was conducted with Cluster software using Pearson's correlation distance metric and average linkage followed by visualization in Treeview software.

Histologic liver analysis

Noncancerous liver tissue that had been surgically resected from patients with HCC and liver specimens obtained by needle biopsy from the background liver of patients with HCC were fixed in 10% buffered formalin and embedded in paraffin. Each paraffin-embedded specimen was sliced into 3 to 4 μm sections and stained with hematoxylin and eosin. Each specimen was semiquantitatively analyzed by assigning a score according to each of the following features: (i) severity of inflammatory cell infiltration (0 for none, 1 for minimal, 2 for mild, 3 for moderate, and 4 for severe) in the periportal, intralobular, and portal areas; (ii) the severity of the F stage of fibrosis (0 for F0, 1 for F1, 2 for F2, 3 for F3, and 4 for F4; ref. 25); the degree of lymphoid aggregates in the portal area (0 for none, 1 for mild, 2 for scattered, 3 for clustered, 4 for lymph follicle without germinal center, and 5 for lymph follicle with germinal center); the severity of portal sclerotic change, perivenular fibrosis, and pericellular fibrosis (on a scale of 0–4 with 0 for none to 4 for severe); the severity of damage to the bile duct (on a scale of 0–4 with 0 for none to 4 for disappearance); the existence of bridging necrosis (0 for none and 1 for existence); the severity of irregular regeneration of hepatocytes as described previously (on a scale of 0–4 with 0 for none to 4 for severe; ref. 26); the grade of steatosis (on a scale of 0–4 with 0 for none to 4 for severe). The irregular regeneration score was based on the findings of a map-like distribution, anisocytosis, and pleomorphism

Published OnlineFirst February 20, 2013; DOI: 10.1158/1078-0432.CCR-12-1641

of the hepatocytes, bulging of the regenerated hepatocytes and proliferation of atypical hepatocytes and oncocytes.

Immunohistochemistry

Paraffin-embedded specimens were sliced into 3 to 4 μm sections, deparaffinized, and subjected to heat-induced epitope retrieval at 98°C for 40 minutes. After blocking endogenous peroxidase activity using 3% hydrogen peroxide, the slide was incubated with appropriately diluted primary antibodies. Antihuman CD4, antihuman CD8 and antihuman CD14 mouse monoclonal antibodies were used to evaluate the immunoreactivity of HCC using a DAKO EnVision+TM kit, as described in the manufacturer's instructions.

We semiquantitatively analyzed tumor tissues by assigning a score to the severity of CD4-positive and CD8-positive lymphocyte infiltration in the tumor tissue (0 for none, 1 for mild, 2 for moderate, and 3 for severe).

Statistical analysis

Fisher exact probability test was used to compare categorical variables and the Mann–Whitney *U* test was used to compare continuous variables; a *P* value of less than 0.05 was considered statistically significant. The TTR survival curve was analyzed using the Kaplan–Meier curve and compared by the log-rank test. Univariate Cox regression analysis was conducted to identify TTR predictors out of clinical and biologic parameters [sex, age, *IL-28B* genotype, therapy, platelet count, alanine aminotransferase (ALT), γ-GTP, albumin, prothrombin activity, bilirubin, Child–Pugh class, history of IFN therapy, AFP, and des-γ-carboxy prothrombin (DCP)] and tumor factors (size and number).

Multivariate analysis was conducted using the Cox regression model with backward elimination (27). The significance level for removing a factor from the model was set to 0.05. A bootstrap technique was applied to confirm the choice of variables (27). One thousand bootstrap samples were generated using resampling with replacement and Cox regression analysis with backward elimination was applied to each sample. The percentage of samples (from the total of 1,000) for which each variable was included in the model was calculated. In multivariate analysis, we evaluated two models that contained either Child–Pugh class or its components to avoid multicollinearity. Data analysis was conducted with R software. We used functions from the Regression Modeling Strategies library for validation with the bootstrap technique (28).

Results

Patient characteristics and *IL-28B* genotype frequency

We genotyped 183 patients with HCC for the *IL-28B* rs8099917 TT, TG, and GG genotypes and observed respective proportions of 67.8% (124 of 183), 30.6% (56 of 183), and 1.6% (3 of 183), which is a similar distribution to that observed in several Japanese studies of patients with CHC (13, 14, 29, 30). Although the prevalence of the TG/GG genotype was higher than that of the general population (12%–16%; refs. 12, 31, 32), there was no significant difference between our result and that of HCV-infected patients in a previous study. There was also no significant difference in clinical variables between the TT and TG/GG genotypes (Table 1).

We next genotyped 160 of 183 cases for rs12979860 and our findings were largely in concordance with those of rs8099917, with the exception of 1 case (0.6%). The haplotype of the case showed that rs8099917 was TT and rs12979860 was CT suggesting that these 2 loci are in a haplotype block with a high level of linkage disequilibrium, as previously reported (13, 30). Genotype distribution analysis showed that rs8099917 was in Hardy–Weinberg equilibrium, so we selected it for further investigation.

During the median follow-up period of 2.5 years (range, 0.3–7.2 years), 118 of 183 patients developed HCC recurrence. Local tumor progression was seen in 13 patients treated by RFA and in only 1 patient treated by resection. The local tumor progression rate and distant recurrence rate were 2.6% and 21.2% in the first year and 8.3% and 54.2% within 2.5 years, respectively. These results are comparable with previous reports by others (33, 34). The type of recurrence was also comparable between *IL-28B* genotype groups.

Associations between the *IL-28B* genotype and HCC clinical outcome

HCC TTR was also analyzed using multivariate Cox regression analysis using 15 clinical parameters and the *IL-28B* genotype. With a significance level of 0.05 for removing a variable in a Cox regression with backward elimination, the *IL-28B* genotype was selected as the final model (Table 2). To confirm this decision, a bootstrapping technique was applied. The percentages of inclusion among the 1,000 samples created by the bootstrapping technique for variables are shown in Table 2. The percentage of inclusion for the *IL-28B* genotype was 80.4%. Frequencies of another variable were lower than 40%. The bootstrap procedure result confirmed the variables chosen for the final model.

In univariate Cox regression analyses, the *IL-28B* genotype was associated with HCC recurrence (Table 2). The TTR survival curve was analyzed using the Kaplan–Meier curve and log-rank test (Fig. 1), and patients with the *IL-28B* TT genotype showed a significantly shorter median TTR (1.61 years) than those with the *IL-28B* TG/GG genotype (2.58 years; $P = 0.007$).

Histologic analysis of noncancerous liver tissues of *IL-28B* TT and TG/GG genotypes

To clarify the molecular mechanism influencing HCC recurrence, we histologically analyzed 141 noncancerous liver tissues according to previously published criteria (Table 3; ref. 26). The mean score of the degree of inflammatory cell infiltration in the periportal area was significantly higher in TT genotype patients (2.804) than TG/GG genotype patients (2.513; $P = 0.025$); the degree of inflammatory cell infiltration in the intralobular area was also

Published OnlineFirst February 20, 2013; DOI: 10.1158/1078-0432.CCR-12-1641

Table 2. Cox regression analysis and relative frequency of variables inclusion with $P < 0.05$ (in 1,000 bootstrap samples)

Variables	Univariate		Multivariate		Frequency (%)
	HR (95% CI)	*P*	HR (95%CI)	*P*	
IL-28B allele: major vs. minor	2.674 (1.161–2.627)	0.007	2.674 (1.161–2.627)	0.007	80.4
Tumor size, mm: >20 vs. ≤20	1.303 (0.881–1.880)	0.193			39.8
AFP, ng/mL: >20 vs. ≤20	1.674 (0.948–1.968)	0.094			33.2
γ-GTP, IU/L: >50 vs. ≤50	1.188 (0.865–1.804)	0.235			32.8
Therapy: RFA vs. resection	1.218 (0.826–2.266)	0.223			31.6
DCP, AU/L: >40 vs. ≤40	1.524 (0.920–1.945)	0.127			27.4
ALT, IU/L: >40 vs. ≤40	0.277 (0.721–1.544)	0.782			23.6
Child–Pugh class: A vs. B	0.025 (0.653–1.515)	0.980			19.2
Period of therapy: 2000-05 vs. 2006-12	0.886 (0.818–1.701)	0.375			15.8
History of IFN therapy: yes vs. no	0.570 (0.771–1.605)	0.569			15.8
Sex: male vs. female	0.108 (0.697–1.496)	0.914			14.6
Tumor number: solitary vs. 2-3	0.263 (0.845–1.857)	0.263			13.4
Platelet count ($\times 10^4/mm^3$): >10 vs. ≤10	0.118 (0.680–1.407)	0.906			12.6
Age: per 1 y	0.621 (0.986–1.028)	0.534			8.4

higher in the TT genotype (2.522) than the TG/GG genotype (2.308), although this did not reach statistical significance ($P = 0.08$). Furthermore, the mean score of the degree of hepatocyte anisocytosis was significantly higher in the TT genotype (1.891) than the TG/GG genotype (1.385; $P = 0.024$). Anisocytosis is characterized by viability of cell size with focal dysplastic change and indicates irregular regeneration of hepatocytes. The irregular regeneration score was higher in the TT genotype (2.207) than the TG/GG genotype (1.795), albeit not significantly ($P = 0.105$).

IL-28B TT and TG/GG genotype gene expression profiles in the noncancerous liver

We next compared the gene expression profile of HCC tissues and noncancerous liver tissues of both the *IL-28B* TT and *IL-28B* TG/GG genotype. Ten patients with HCC were selected from each *IL-28B* genotype and their gene expression was determined using Affymetrix genechip analysis (Supplementary Table S1). We recently reported that expression of hepatic ISGs is downregulated in individuals with the *IL-28B* TT genotype, whereas the expression of other immune response-related genes was shown to be upregulated (13). Therefore, to validate our expression data, we compared the expression of ISGs and other immune response-related genes in the present study with that of the previous study. We analyzed the expression data of 20 patients from the current study in addition to another series of 91 patients with CHC from our previous study.

One-way hierarchical clustering using 28 representative ISGs showed that patients with the *IL-28B* TG/GG genotype

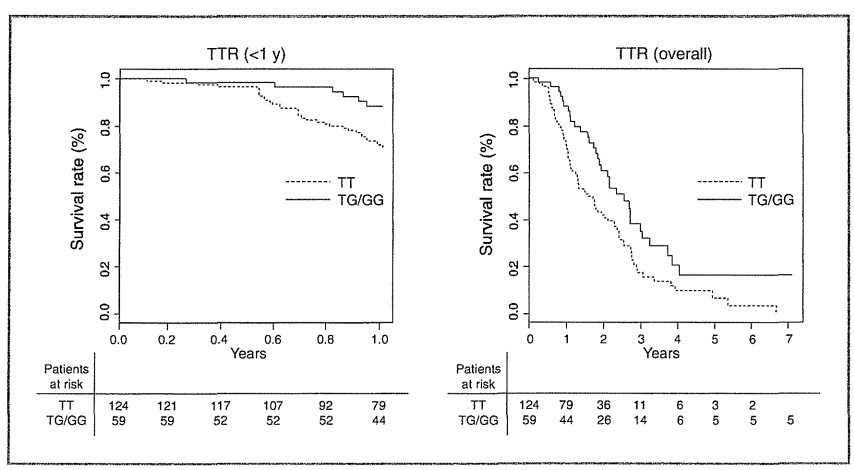

Figure 1. Kaplan–Meier curves of early and overall TTR in relation to *IL-28B* genotype. The patients with the *IL-28B* TT genotype showed a significantly shorter median TTR (1.61 years) than those with the *IL-28B* TG/GG genotype (2.58 years; $P = 0.007$).

Published OnlineFirst February 20, 2013; DOI: 10.1158/1078-0432.CCR-12-1641

Table 3. Comparison of liver histology between *IL-28B* major and minor genotypes

Variable	*IL-28B* TT genotype ($n = 92$)	*IL-28* TG/GG genotype ($n = 39$)	*P* value
Score of inflammatory cell infiltration			
Periportal	2.804	2.513	0.032
Intralobular	2.522	2.308	0.082
Portal	2.946	2.846	0.322
Fibrosis	3.587	3.436	0.428
Portal lymphoid reaction	4.098	3.949	0.363
Damage of bile duct	0.380	0.256	0.216
Portal sclerotic change	0.076	0.077	0.990
Perivenular fibrosis	1.133	1.000	0.447
Pericellular fibrosis	1.163	0.821	0.045
Bridging fibrosis	0.957	0.641	0.106
Irregular regeneration	2.207	1.795	0.105
Anisocytosis	1.891	1.385	0.024
Bulging	0.326	0.436	0.485
Map-like distribution	1.370	1.333	0.881
Oncocytes	1.326	1.051	0.227
Nodularity	1.185	1.231	0.849
Atypical hepatocytes	0.467	0.692	0.304
Steatosis	1.707	1.692	0.951

NOTE: Data shown as mean.

had higher expression of hepatic ISGs, whereas patients with the TT genotype showed lower expression of hepatic ISGs in CHC tissues and noncancerous background liver tissue, confirming our previous data (Fig. 2A and Supplementary Table S2). Expression of hepatic ISGs in HCC tissues was lower than in background liver tissues, with no relationship to the *IL-28B* genotype. Hierarchical clustering of 51 representative immune response-related genes from the Gene Ontology gene set of the Molecular Signatures Database indicated that their expression was upregulated in TT genotype compared with TG/GG genotype tissues, with the exception of HCC tissues (Fig. 2B and Supplementary Table S2). Upregulation of immune response-related genes suggests that hepatic inflammation is more severe in TT genotype patients, which is consistent with our histologic findings and recent studies that reported an association between high serum ALT levels and the *IL-28B* TT genotype (14, 29).

Gene expression profile of HCC tissues from *IL-28B* TT and TG/GG genotypes

We applied PAGE to identify gene sets differentially regulated between the different *IL-28B* genotypes from the whole gene expression profiles derived from HCC tissues. Analysis of groups of genes involved in a specific function enables significant differences to represent a biologically meaningful result (23). Many gene sets associated with the immune system (e.g., the immune system process, T-cell activation, regulation of T-cell activation, and T-cell proliferation) showed a significant increase in their expression in patients with HCC with the *IL-28B* TG/GG genotype (Supplementary Table S3). This PAGE profile was consistent with the hierarchical clustering of 51 immune response-related genes (Fig. 2B) and suggests that the immune response to tumors might be more intensive in *IL-28B* TG/GG genotype HCC than *IL-28B* TT genotype HCC.

Lymphocyte infiltration into HCC tissues with the *IL-28B* TG/GG genotype

To verify our PAGE profile, we histologically compared HCC tissue of 20 cases of the *IL-28B* TT genotype and 12 cases of the TG/GG genotype using immunohistochemical staining with antibodies against helper T cells (CD4) and cytotoxic T cells (CD8). The mean score of the degree of $CD8^+$ lymphocyte infiltration in the tumor tissue was significantly higher in the TG/GG genotype (1.75) than the TT genotype (1.175; $P = 0.047$; Supplementary Table S4). A representative case is shown in Fig. 3. There was no morphologic alteration associated with the *IL-28B* genotype. Immunohistochemical analysis showed intratumoral infiltration of $CD4^+$ and $CD8^+$ lymphoid cells and slight infiltration of monocytes/macrophages in HCC of the *IL-28B* TG/GG genotype, compared with little infiltration of lymphocytes or monocytes/macrophages in HCC of the *IL-28B* TT genotype.

Furthermore, the gene set differentially expressed in HCC-infiltrating mononuclear inflammatory cells from our previous study (24) was upregulated in HCC of the *IL-28B* TG/GG genotype (Z score, −9.879; $P < 0.001$). One-way hierarchical clustering was carried out of 122 genes involved in the gene set differentially expressed in HCC-infiltrating

Published OnlineFirst February 20, 2013; DOI: 10.1158/1078-0432.CCR-12-1641

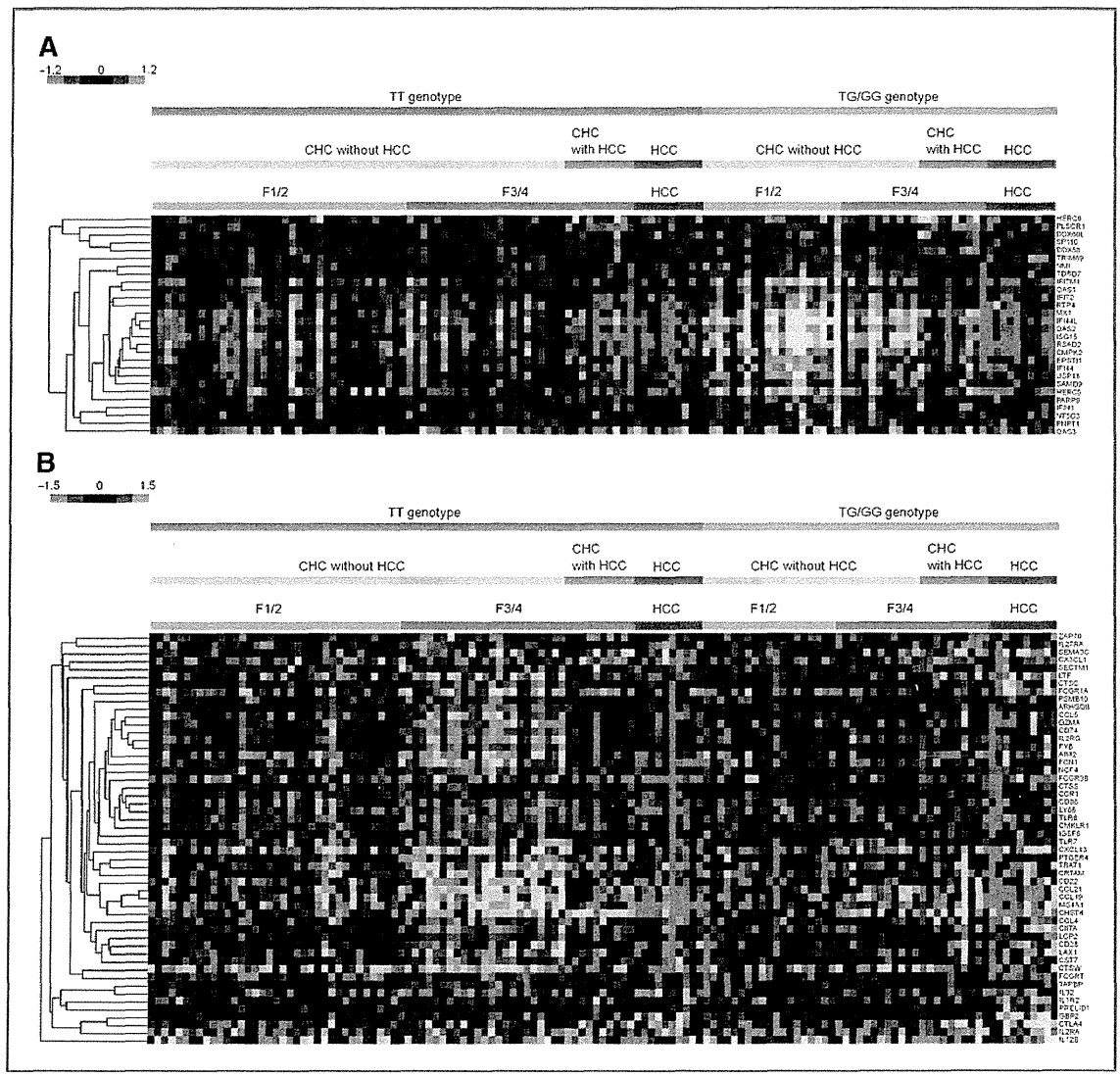

Figure 2. A, one-way hierarchical clustering of 28 representative ISGs of 111 patients with the *IL-28B* genotype. B, one-way hierarchical clustering analysis of 51 representative immune response-related genes of 111 patients with the *IL-28B* genotype.

mononuclear inflammatory cells. Most of the 122 genes were expressed at high levels in many HCC tissues of *IL-28B* TG/GG genotype patients (Supplementary Fig. S2).

Discussion

IL-28B is a recently identified, novel IFN-λ family member that shares the same biologic properties as type I IFNs (9). Recent reports have shown a significant association between *IL-28B* allelic variants and treatment outcome in CHC (11, 12). *IL-28B* genotyping is therefore considered to be a suitable pretreatment predictor of treatment response for individual patients, and also an indicator of biochemical and histologic findings in patients infected with HCV (14). In this study, we determined that the *IL-28B* genotype is associated with HCC recurrence in patients with CHC as patients with the *IL-28B* TT genotype showed a significantly higher incidence of recurrence than those with the *IL-28B* TG/GG genotype after curative therapy. To our knowledge, this is the first study to reveal an association between the *IL-28B* genotype and HCC recurrence and molecular features in patients with CHC.

To date, there are several contradicting results about the association of the *IL-28B* genotype and progression of liver disease including the development of HCC. Fabris and colleagues and Eurich and colleagues reported that

Published OnlineFirst February 20, 2013; DOI: 10.1158/1078-0432.CCR-12-1641

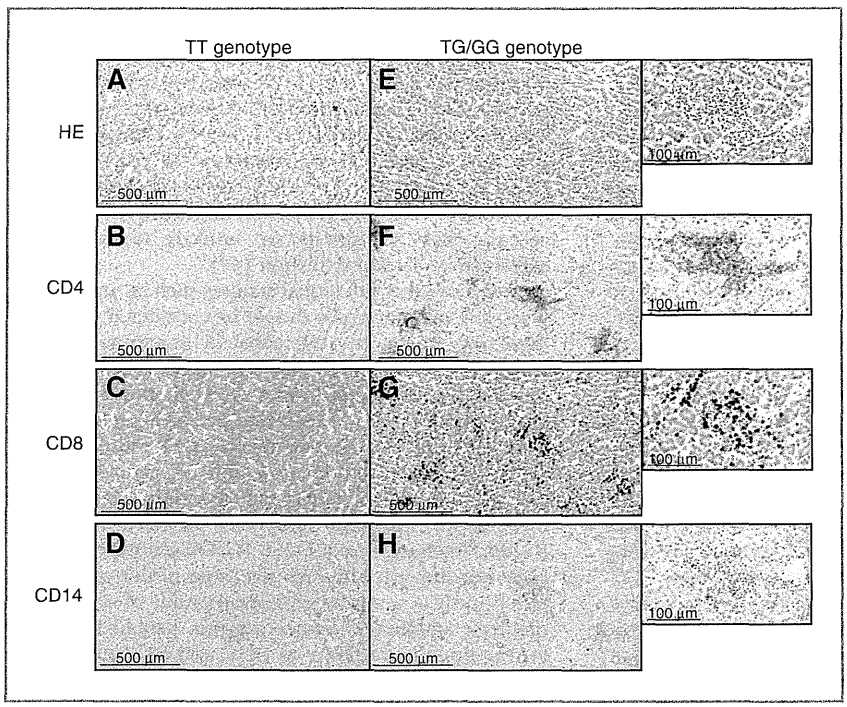

Figure 3. Expression of CD4, CD8, and CD14 in tumor-infiltrating mononuclear cells in HCC tissues. Immunohistochemical analysis of noncancerous liver tissues of *IL-28B* TT (A–D) and TG/GG genotypes (E–H). Samples were analyzed by hematoxylin and eosin staining (A and E), CD4 staining (B and F), CD8 staining (C and G), and CD14 staining (D and H).

patients with a T allele in rs12979860 (G allele in rs8099917) were at a high risk of progressing to liver cirrhosis and HCC (35, 36), however, these reports have not yet been confirmed by others. A large-scale European genome-wide association study (GWAS) recently identified a weak protective role for the rs12979860 T allele in the progression of fibrosis during HCV infection (37), whereas a Japanese GWAS identifying a susceptibility locus for HCV-induced HCC found no association of rs12979860 and rs8099917 SNPs with HCC (38). In support of these findings, Joshita and colleagues reported no association between the *IL-28B* genotype and the incidence of primary HCC (39). These results show a good concordance with those of the present study, which revealed that the *IL-28B* genotype was not associated with HCC incidence before treatment (Table 1). Furthermore, closer histologic assessment showed a high score of periportal inflammation and pericellular fibrosis in the rs8099917 TT genotype (CC in rs12979860). This suggests that our patient selection process was not biased, and that our results are in agreement with the Japanese study and are comparable with the European study.

To date, the reasons for contradicting results about the association of the *IL-28B* genotype and progression of liver disease have not been clear, however, clinical bias such as patient number, history of treatment, virus genotype, and titer and racial differences may affect the results. It should be noted that significant differences in genotype frequencies with respect to ethnic/racial groups have previously been reported for *IL-28B* SNPs (11). To overcome these limitations, a future cross-sectional prospective study should be conducted.

Several risk factors for HCC recurrence have previously been reported, including the presence of cirrhosis, high AFP levels, and multiplicity of tumors 7, 8). However, multivariate analysis and the bootstrap procedure of the present study revealed that the *IL-28B* genotype was independent indicators for recurrence, suggesting that it is stronger predictors of HCC recurrence than other factors.

The expression of hepatic ISGs was higher in *IL-28B* TG/GG genotype patients than *IL-28B* TT genotype patients with CHC in this study. This confirms our previous findings in a different cohort and those of another research group (13, 40). Several ISGs have been reported to have antiproliferative and proapoptotic functions (41, 42), and IFN-α (type I IFN) has also been found to inhibit metastasis and human HCC recurrence after curative resection mediated by angiogenesis (43). Indeed, *IL-28B* rs8099917 is associated with early HCC recurrence (<1 year), possibly because of the intrahepatic metastasis of HCC in this study (Fig. 1 and Supplementary Table S5). These reports and our findings suggest that high expression of hepatic ISGs might cause the low HCC recurrence in the *IL-28B* TG/GG genotype, although the mechanism of this association remains unknown.

Microarray, histologic, and immunohistochemical analysis in the present study showed that the immune response was more severe in chronic hepatitis and noncancerous tissue of *IL-28B* TT genotype compared with TG/GG genotype patients. Serum ALT levels were also higher in the

Published OnlineFirst February 20, 2013; DOI: 10.1158/1078-0432.CCR-12-1641

IL-28B TT genotype, albeit not significantly. These results support previous findings that showed higher serum ALT levels and more severe liver inflammation in TT genotype compared with TG/GG genotype patients with HCC (14, 29). Irregular regeneration of hepatocytes develops as a result of repeated cycles of necrosis and regeneration of hepatocytes and was previously reported to be an important predictive factor for the development of HCC (26). We histologically showed that the degree of hepatocyte anisocytosis was more severe in noncancerous livers of TT genotype than TG/GG genotype patients, perhaps because of *IL-28B* genotype-dependent hepatic inflammation. This might also affect the late recurrence of HCC (>1 year) as a result of the multicentric occurrence of HCC in background liver disease. In the late recurrence group, *IL-28B* TT genotype patients showed a shorter TTR than *IL-28B* TG/GG genotype patients although this did not reach statistical significance ($P = 0.086$; Supplementary Fig. S3; Supplementary Table S6).

Previous studies showed that the gene expression profile of noncancerous liver tissue was associated with late recurrence HCC and the multicentric occurrence of HCC (44). However, the gene set expression of these studies did not differ between the *IL-28B* TT and TG/GG genotypes in the present study. Although the reason for this discrepancy is unclear, the *IL-28B* genotype may affect early recurrence more than late recurrence, and the limited number of patients and the short follow-up period may affect statistical comparisons. Therefore, further investigations with a large series of patients are necessary to clarify whether *IL-28B* genotype-dependent inflammation influences HCC recurrence.

On the other hand, the gene expression profile and histologic analyses showed that more lymphocytes infiltrate into the tumor tissue of the *IL-28B* TG/GG genotype than the TT genotype. Chew and colleagues previously showed that 14 intratumoral immune gene signatures were able to identify molecular cues driving the tumor infiltration of lymphocytes and predict the survival of patients with HCC, particularly during the early stages of disease (45). We can confirm that the expression of some of these 14 genes was higher in TG/GG genotype than TT genotype patients (Supplementary Fig. S4), supporting the association of the *IL-28B* genotype, HCC recurrence, and histologic findings. The presence of lymphocyte infiltration in HCC was also reported as a negative predictor of HCC recurrence after liver transplantation (46), and this phenomenon may contribute to a lower incidence of HCC recurrence in the TG/GG genotype.

It may seem contradictory that the immune response in noncancerous liver was more severe in TT genotype than TG/GG genotype patients despite the fact that the expression of immune genes was higher in tumor tissue and more lymphocytes infiltrated the tumor in the TG/GG genotype compared with the TT genotype. Although we are unable to explain this contradiction, it is conceivable that the host immune reaction has a differential role between tumor and nontumor tissue. Moreover, HCV-specific T-cell immune responses, which are essential for disease control, are attenuated in patients with CHC, and T-cell exhaustion has recently been implicated in the deficient control of chronic viral infections. On the other hand, little is known on self- and tumor-specific T-cell responses in patients with HCC. While several reports have shown the existence of exhausted T cells in a tumor environment, impaired T-cell responses to tumors are unlikely to be simply explained by T-cell exhaustion (47).

Anergy or other functional statuses such as suppressive immunity by tumor cells should be considered in tumor immunity. Therefore, differences in immunity to viral antigens and self- and tumor-antigens could explain our findings, although further work should be carried out to confirm these conclusions. We have preliminarily confirmed that the ratio of regulatory T cells is higher in the peripheral blood of *IL-28B* TT genotype HCC patients than *IL-28B* TG/GG genotype patients, although there is no significant difference between non-HCC *IL-28B* TT genotype and *IL-28B* TG/GG genotype patients (data not shown). Although the cause of this phenomenon is unclear, our gene expression profile of noncancerous liver and tumor tissues suggests paradoxical roles for the immune response in CHC and HCC depending on *IL-28B* genotype; it will be necessary to clarify these mechanisms in future investigations.

Recently, a sustained virologic response (SVR) to CHC antiviral treatment was shown to be associated with a lower risk of HCC recurrence (48). Although we did not include patients with SVR in the current study, we nevertheless observed that they showed a longer recurrence-free survival than patients infected with HCV, independent of *IL-28B* genotype (data not shown). This result together with the association between the *IL-28B* genotype and response to antiviral treatment promotes recommendations for aggressive CHC antiviral treatment, especially in cases with the *IL-28B* TT genotype.

RFA is a recently developed technique and its efficacy has been reported equal to that of surgical resection, especially in early-stage HCC (3–6). In the European Association for the Study of the Liver–European Organisation for Research and Treatment of Cancer (EASL-EORTC) guidelines, RFA is considered the standard care for patients with Barcelona Clinic Liver Cancer stage 0-A tumors not suitable for surgery and whether or not RFA can be considered a competitive alternative to resection is uncertain (49). In our study, the local tumor progression rate was not statistically different between RFA and resection cases. However, further studies with an appropriate sample population are necessary to clarify the comparison of RFA and resection. The present study has some limitations. It was a retrospective cohort and a single-center study, so it was difficult to completely eliminate bias. Further prospective studies of a larger series of patients should be conducted to validate our results. As a consequence of the small sample size and even smaller number of patients undergoing surgical resection, we could not show an association between *IL-28B* genotype and HCC

Published OnlineFirst February 20, 2013; DOI: 10.1158/1078-0432.CCR-12-1641

recurrence in the surgical resection group (data not shown). However, we did find no significant difference in TTR between RFA and surgical resection, confirming previous findings.

In conclusion, we found that the *IL-28B* rs8099917 TT genotype is associated with shorter TTR in patients with HCC with CHC. Microarray analysis showed a high expression of ISGs in background liver and high expression of immune system-related genes in tumor tissues of the *IL-28B* TG/GG genotype. Histologic findings also showed that more lymphocytes infiltrated into tumor tissues in the TG/GG genotype. The *IL-28B* genotype therefore is a candidate useful genetic marker to predict HCC recurrence as well as the response to pegylated-IFN and ribavirin combination therapy for CHC.

Disclosure of Potential Conflicts of Interest

No potential conflicts of interest were disclosed.

Authors' Contributions

Conception and design: M. Honda, Y. Sakai, M. Moriyama, S. Kaneko
Development of methodology: M. Moriyama
Acquisition of data (provided animals, acquired and managed patients, provided facilities, etc.): Y. Hodo, A. Tanaka, K. Arai, T. Yamashita, T. Yamashita, A. Sakai, Y. Nakanuma, M. Moriyama, S. Kaneko
Analysis and interpretation of data (e.g., statistical analysis, biostatistics, computational analysis): Y. Hodo, M. Honda, M. Sasaki, M. Moriyama
Writing, review, and/or revision of the manuscript: Y. Hodo, M. Honda, M. Moriyama
Administrative, technical, or material support (i.e., reporting or organizing data, constructing databases): Y. Hodo, A. Tanaka, Y. Nomura, K. Arai, E. Mizukoshi, M. Sasaki, M. Moriyama, S. Kaneko
Study supervision: Y. Sakai, E. Mizukoshi, M. Moriyama

The costs of publication of this article were defrayed in part by the payment of page charges. This article must therefore be hereby marked *advertisement* in accordance with 18 U.S.C. Section 1734 solely to indicate this fact.

Received May 25, 2012; revised December 20, 2012; accepted February 7, 2013; published OnlineFirst February 20, 2013.

References

1. Yang JD, Roberts LR. Hepatocellular carcinoma: a global view. Nat Rev Gastroenterol Hepatol 2010;7:448–58.
2. Cha C, DeMatteo RP, Blumgart LH. Surgery and ablative therapy for hepatocellular carcinoma. J Clin Gastroenterol 2002;35(5 Suppl 2): S130–7.
3. Lü M, Kuang M, Liang L, Xie X, Peng B, Liu G, et al. Surgical resection versus percutaneous thermal ablation for early-stage hepatocellular carcinoma: a randomized clinical trial. Zhonghua Yi Xue Za Zhi 2006; 86:801–5.
4. Chen M-S, Li J-Q, Zheng Y, Guo R-P, Liang H-H, Zhang Y-Q, et al. A prospective randomized trial comparing percutaneous local ablative therapy and partial hepatectomy for small hepatocellular carcinoma. Ann Surg 2006;243:321–8.
5. Hong SN, Lee S-Y, Choi MS, Lee JH, Koh KC, Paik SW, et al. Comparing the outcomes of radiofrequency ablation and surgery in patients with a single small hepatocellular carcinoma and well-preserved hepatic function. J Clin Gastroenterol 2005;39: 247–52.
6. Nishikawa H, Inuzuka T, Takeda H, Nakajima J, Matsuda F, Sakamoto A, et al. Comparison of percutaneous radiofrequency thermal ablation and surgical resection for small hepatocellular carcinoma. BMC Gastroenterol 2011;11:143.
7. Koike Y, Shiratori Y, Sato S, Obi S, Teratani T, Imamura M, et al. Risk factors for recurring hepatocellular carcinoma differ according to infected hepatitis virus-an analysis of 236 consecutive patients with a single lesion. Hepatology 2000;32:1216–23.
8. Yamanaka Y, Shiraki K, Miyashita K, Inoue T, Kawakita T, Yamaguchi Y, et al. Risk factors for the recurrence of hepatocellular carcinoma after radiofrequency ablation of hepatocellular carcinoma in patients with hepatitis C. World J Gastroenterol 2005;11:2174–8.
9. Sheppard P, Kindsvogel W, Xu W, Henderson K, Schlutsmeyer S, Whitmore TE, et al. IL-28, IL-29 and their class II cytokine receptor IL-28R. Nat Immunol 2003;4:63–8.
10. Li M, Liu X, Zhou Y, Su SB. Interferon-lambdas: the modulators of antivirus, antitumor, and immune responses. J Leukoc Biol 2009; 86:23–32.
11. Ge D, Fellay J, Thompson AJ, Simon JS, Shianna KV, Urban TJ, et al. Genetic variation in IL28B predicts hepatitis C treatment-induced viral clearance. Nature 2009;461:399–401.
12. Tanaka Y, Nishida N, Sugiyama M, Kurosaki M, Matsuura K, Sakamoto N, et al. Genome-wide association of IL28B with response to pegylated interferon-alpha and ribavirin therapy for chronic hepatitis C. Nat Genet 2009;41:1105–9.
13. Honda M, Sakai A, Yamashita T, Nakamoto Y, Mizukoshi E, Sakai Y, et al. Hepatic ISG expression is associated with genetic variation in interleukin 28B and the outcome of IFN therapy for chronic hepatitis C. Gastroenterology 2010;139:499–509.
14. Abe H, Ochi H, Maekawa T, Hayes CN, Tsuge M, Miki D, et al. Common variation of IL28 affects gamma-GTP levels and inflammation of the liver in chronically infected hepatitis C virus patients. J Hepatol 2010;53:439–43.
15. Rauch A, Kutalik Z, Descombes P, Cai T, Di Iulio J, Mueller T, et al. Genetic variation in IL28B is associated with chronic hepatitis C and treatment failure: a genome-wide association study. Gastroenterology 2010;138:1338–45, 1345.e1–7.
16. Kudo M, Okanoue T. Management of hepatocellular carcinoma in Japan: consensus-based clinical practice manual proposed by the Japan Society of Hepatology. Oncology 2007;72(Suppl 1):2–15.
17. Kokudo N, Makuuchi M. Evidence-based clinical practice guidelines for hepatocellular carcinoma in Japan: the J-HCC guidelines. J Gastroenterol 2009;44(Suppl 1):119–21.
18. Matsui O. Imaging of multistep human hepatocarcinogenesis by CT during intra-arterial contrast injection. Intervirology 2004;47:271–6.
19. Liver Cancer Study Group of Japan. The general rules for the clinical and pathological study of primary liver cancer. 5th ed. Tokyo, Japan: Kanahara Shuppan; 2009.
20. R Development Core Team. R: a language and environment for statistical computing. Vienna, Austria: R Foundation for Statistical Computing; 2012. [cited 2012 May 1]. Available from: http://www.r-project.org/.
21. Gentleman RC, Carey VJ, Bates DM, Bolstad B, Dettling M, Dudoit S, et al. Bioconductor: open software development for computational biology and bioinformatics. Genome Biol 2004;5:R80.
22. Subramanian A, Tamayo P, Mootha VK, Mukherjee S, Ebert BL, Gillette MA, et al. Gene set enrichment analysis: a knowledge-based approach for interpreting genome-wide expression profiles. Proc Natl Acad Sci U S A 2005;102:15545–50.
23. Kim S-Y, Volsky DJ. PAGE: parametric analysis of gene set enrichment. BMC Bioinformatics. 2005;6:144.
24. Sakai Y, Honda M, Fujinaga H, Tatsumi I, Mizukoshi E, Nakamoto Y, et al. Common transcriptional signature of tumor-infiltrating mononuclear inflammatory cells and peripheral blood mononuclear cells in hepatocellular carcinoma patients. Cancer Res 2008;68:10267.
25. Desmet VJ, Gerber M, Hoofnagle JH, Manns M, Scheuer PJ. Classification of chronic hepatitis: diagnosis, grading and staging. Hepatology 1994;19:1513–20.

Published OnlineFirst February 20, 2013; DOI: 10.1158/1078-0432.CCR-12-1641

26. Ueno Y, Moriyama M, Uchida T, Arakawa Y. Irregular regeneration of hepatocytes is an important factor in the hepatocarcinogenesis of liver disease. Hepatology 2001;33:357–62.
27. Sauerbrei W, Schumacher M. A bootstrap resampling procedure for model building: application to the Cox regression model. Stat Med 1992;11:2093–109.
28. Harrell FE Jr. rms: regression modeling strategies. 2012. [cited 2012 May 1]. Available from: http://cran.r-project.org/package=rms.
29. Akuta N, Suzuki F, Hirakawa M, Kawamura Y, Yatsuji H, Sezaki H, et al. Amino acid substitution in hepatitis C virus core region and genetic variation near the interleukin 28B gene predict viral response to telaprevir with peginterferon and ribavirin. Hepatology 2010;52:421–9.
30. Miyamura T, Kanda T, Nakamoto S, Wu S, Fujiwara K, Imazeki F, et al. Hepatic STAT1-nuclear translocation and interleukin 28B polymorphisms predict treatment outcomes in hepatitis C virus genotype 1-infected patients. PLoS ONE 2011;6:e28617.
31. Ochi H, Maekawa T, Abe H, Hayashida Y, Nakano R, Imamura M, et al. IL-28B predicts response to chronic hepatitis C therapy—fine-mapping and replication study in Asian populations. J Gen Virol 2011;92:1071–81.
32. Database of single nucleotide polymorphisms (dbSNP). Bethesda, MD: National Center for Biotechnology Information, National Library of Medicine. dbSNP accession:rs8099917 (dbSNP Build ID: 137). [cited 2012 Oct 1]. Available from: http://www.ncbi.nlm.nih.gov/SNP/.
33. Shiina S, Tateishi R, Arano T, Uchino K, Enooku K, Nakagawa H, et al. Radiofrequency ablation for hepatocellular carcinoma: 10-year outcome and prognostic factors. Am J Gastroenterol 2012;107:569–77.
34. Lencioni R, Cioni D, Crocetti L, Franchini C, Pina C Della, Lera J, et al. Early-stage hepatocellular carcinoma in patients with cirrhosis: long-term results of percutaneous image-guided radiofrequency ablation. Radiology 2005;234:961–7.
35. Fabris C, Falleti E, Cussigh A, Bitetto D, Fontanini E, Bignulin S, et al. IL-28B rs12979860 C/T allele distribution in patients with liver cirrhosis: role in the course of chronic viral hepatitis and the development of HCC. J Hepatol 2011;54:716–22.
36. Eurich D, Boas-Knoop S, Bahra M, Neuhaus R, Somasundaram R, Neuhaus P, et al. Role of IL28B polymorphism in the development of hepatitis C virus-induced hepatocellular carcinoma, graft fibrosis, and posttransplant antiviral therapy. Transplantation 2012;93:644–9.
37. Patin E, Kutalik Z, Guergnon J, Bibert S, Nalpas B, Jouanguy E, et al. Genome-wide association study identifies variants associated with progression of liver fibrosis from HCV infection. Gastroenterology 2012;143:1244–52.e12.
38. Kumar V, Kato N, Urabe Y, Takahashi A, Muroyama R, Hosono N, et al. Genome-wide association study identifies a susceptibility locus for HCV-induced hepatocellular carcinoma. Nat Genet 2011;43:455–8.
39. Joshita S, Umemura T, Katsuyama Y, Ichikawa Y, Kimura T, Morita S, et al. Association of IL28B gene polymorphism with development of hepatocellular carcinoma in Japanese patients with chronic hepatitis C virus infection. Hum Immunol 2012;73:298–300.
40. Urban TJ, Thompson AJ, Bradrick SS, Fellay J, Schuppan D, Cronin KD, et al. IL28B genotype is associated with differential expression of intrahepatic interferon-stimulated genes in patients with chronic hepatitis C. Hepatology 2010;52:1888–96.
41. Besch R, Poeck H, Hohenauer T, Senft D, Häcker G, Berking C, et al. Proapoptotic signaling induced by RIG-I and MDA-5 results in type I interferon-independent apoptosis in human melanoma cells. J Clin Invest 2009;119:2399–411.
42. Stawowczyk M, Van Scoy S, Kumar KP, Reich NC. The interferon stimulated gene 54 promotes apoptosis. J Biol Chem 2011;286:7257–66.
43. Wang L, Wu W-Z, Sun H-C, Wu X-F, Qin L-X, Liu Y-K, et al. Mechanism of interferon alpha on inhibition of metastasis and angiogenesis of hepatocellular carcinoma after curative resection in nude mice. J Gastrointest Surg 2003;7:587–94.
44. Hoshida Y, Villanueva A, Kobayashi M, Peix J, Chiang DY, Camargo A, et al. Gene expression in fixed tissues and outcome in hepatocellular carcinoma. N Engl J Med 2008;359:1995–2004.
45. Chew V, Chen J, Lee D, Loh E, Lee J, Lim KH, et al. Chemokine-driven lymphocyte infiltration: an early intratumoural event determining long-term survival in resectable hepatocellular carcinoma. Gut 2012;61:427–38.
46. Unitt E, Marshall A, Gelson W, Rushbrook SM, Davies S, Vowler SL, et al. Tumour lymphocytic infiltrate and recurrence of hepatocellular carcinoma following liver transplantation. J Hepatol 2006;45:246–53.
47. Baitsch L, Baumgaertner P, Devêvre E, Raghav SK, Legat A, Barba L, et al. Exhaustion of tumor-specific $CD8^+$ T cells in metastases from melanoma patients. J Clin Invest 2011;121:2350–60.
48. Miyatake H, Kobayashi Y, Iwasaki Y, Nakamura S-I, Ohnishi H, Kuwaki K, et al. Effect of previous interferon treatment on outcome after curative treatment for hepatitis C virus-related hepatocellular carcinoma. Dig Dis Sci 2012;57:1092–101.
49. European Association For The Study Of The Liver; European Organisation For Research And Treatment Of Cancer. EASL-EORTC clinical practice guidelines: management of hepatocellular carcinoma. J hepatol 2012;56:908–43.

Cellular Immunology 282 (2013) 44–52

Contents lists available at SciVerse ScienceDirect

Cellular Immunology

journal homepage: www.elsevier.com/locate/ycimm

ER stress induced impaired TLR signaling and macrophage differentiation of human monocytes

Takuya Komura [a,1], Yoshio Sakai [b,1], Masao Honda [a], Toshinari Takamura [a], Takashi Wada [b], Shuichi Kaneko [a,*]

[a] Disease Control and Homeostasis, Kanazawa University, 13-1, Takaramachi, Kanazawa 920-8641, Japan
[b] Department of Laboratory Medicine, Kanazawa University, 13-1, Takaramachi, Kanazawa 920-8641, Japan

ARTICLE INFO

Article history:
Received 10 September 2012
Accepted 14 April 2013
Available online 24 April 2013

Keywords:
ER stress
Monocyte
TLR signaling
Differentiation

ABSTRACT

Endoplasmic reticulum (ER) stress causes impairment of the intracellular protein synthesis machinery, affecting various organ functions and homeostasis systems, including immunity. We found that ER stress induced by the N-linked glycosylation inhibitor, tunicamycin, caused susceptibility to apoptosis in the human monocytic cell line, THP-1 cells. Importantly, prior to tunicamycin-induced apoptosis, the proinflammatory response to toll-like receptor (TLR) 4 ligand lipopolysaccharide (LPS) stimulation was attenuated with respect to the expression of the proinflammatory cytokines. This impaired expression of proinflammatory cytokines was a consequence of the inhibition of NF-κB activation. Moreover, tunicamycin-induced ER stress disturbed the differentiation of THP-1 cells into macrophages induced by phorbol-12-myristate-13-acetate treatment. We also confirmed that ER stress affected the response of primary human monocytes to TLR ligand and their ability to differentiate into macrophages. These data suggest that ER stress imposes an important pathological insult to the immune system, affecting the crucial functions of monocytes.

1. Introduction

Homeostasis of physiological activities and structural components of the body requires properly functioning cellular machinery, including the components involved in protein synthesis. The endoplasmic reticulum (ER) plays a central role in the synthesis, maturation and assembly of secretary and structural proteins [1], and under some conditions, ER stress can disrupt ER function [2]. ER stress affects physiological cellular activities, disturbing cell-type specific functions or cell viability and inducing apoptosis [3]. ER stress has been observed in a variety of diseases, such as cancer, metabolic diseases, atherosclerosis and neurodegenerative diseases, including Parkinson's disease and Alzheimer's disease [4–7]; however, it is not clear whether ER stress is the cause or consequence of these diseases.

Composed of many cell types, including monocytes, macrophages, dendritic cells (DCs) and lymphocytes, the immune system contributes to homeostasis by protecting the host from exogenous pathogens or harmful unexpected endogenous events, such as cancer. Monocytes are critical immune cells that express pattern-recognition molecules, toll-like receptors (TLRs), important for innate immunity against various pathogens [8,9]. Monocytes are also the progenitors for differentiation into macrophages or DCs, both of which are pivotal regulators of immune reaction [10].

Previously, we observed that human monocytes in patients with diabetes were under ER stress, were functionally impaired regarding TLR signaling and were vulnerable to apoptosis [11]. These observations suggested that ER stress is involved in the impairment of monocytes, thereby compromising host immunity.

In this study, we further examined how ER stress affects monocytes. When primary human monocytes and THP-1 human monocytic cell line cells were stimulated with toll-like receptor (TLR) 4 ligand lipopolysaccharide (LPS), we observed that monocytes were attenuated in their capability to secrete proinflammatory cytokines. Moreover, when cells were under ER stress induced by the N-linked glycosylation inhibitor, tunicamycin, decreased activation of NF-κB was observed. In addition to this functional impairment of cytokine expression, ER stress also impaired monocyte differentiation into macrophages. Interestingly, the TLR4 signaling in differentiated macrophages was also impaired under ER stress. These results demonstrate that ER stress is an important pathological condition that broadly affects monocyte-lineage cells, influencing the innate immune system function of monocytes and macrophages as well as the differentiation capability of progenitor cells for antigen presentation.

* Corresponding author. Address: Disease Control and Homeostasis, Graduate School of Medical Science, Kanazawa, University, Kanazawa 920-8641, Japan. Fax: +81 76 234 4250.
E-mail address: skaneko@m-kanazawa.jp (S. Kaneko).
[1] These authors contributed equally to this work.

0008-8749/$ - see front matter © 2013 Elsevier Inc. All rights reserved.
http://dx.doi.org/10.1016/j.cellimm.2013.04.006

2. Materials and methods

2.1. Human monocytes

THP-1 cells, a human monocytic cell line, were obtained from American Type Culture Collection (Manassas, VA). THP-1 cells were cultured in RPMI1640 culture medium (Invitrogen, Carlsbad, CA) supplemented with 10% heat-inactivated fetal bovine serum (FBS, Invitrogen). Human primary monocytes were obtained from healthy volunteers as follows: peripheral blood mononuclear cells (PBMCs) were freshly isolated from heparinized venous blood using Ficoll–Hypaque (Sigma–Aldrich, St. Louis, MO). $CD14^+$ monocyte subpopulations were isolated using a magnetic cell sorting system in accordance with the manufacturer's protocol (Miltenyi Biotec, Bergisch Gladbach, Germany).

2.2. Induction of macrophage-differentiation

For macrophage differentiation, THP-1 cells were cultured in medium supplemented with Phorbol-12-myristate-13-acetate (PMA) (50 ng/ml) (Sigma–Aldrich) for 72 h. Primary human monocytes were cultured in medium supplemented with GM-CSF (100 ng/ml) (Sigma–Aldrich) for 4 days. Macrophage differentiation was assessed by morphology under microscopic examination and expression of the macrophage-related surface markers, CD11b and CD68, as analyzed by flow cytometry analysis and quantitative real-time detection PCR (RTD-PCR).

2.3. ER stress induction

To induce ER stress, THP-1 cells were treated with 1 or 5 μg/ml of tunicamycin (Sigma–Aldrich) and 3 μM thapsigargin (Sigma–Aldrich) for 12 h. The treated cells were assessed for apoptosis and cytokine expression in response to LPS stimulation.

2.4. Flow cytometry analysis

Flow cytometry analysis was performed as previously reported. For the surface molecule expression, cells were incubated with phycoerythrin (PE)-labeled anti-TLR4 (eBioscience, San Diego, CA), anti- CD11b and CD68 (BD Biosciences, San Jose, CA) in PBS containing 2% bovine serum albumin (BSA) (Sigma–Aldrich). For assessment of apoptosis, cells were incubated with fluorescein isothiocyanate (FITC)-labeled anti-CD14 antibody (BD Bioscience) and with PE-labeled Annexin-V and 7-amino-actinomycin D (7-AAD, Apoptosis Detection Kit I, BD Biosciences). Apoptotic cells were determined by flow cytometry for the fraction of cells labeled with Annexin-V that were 7-AAD negative using a FACSCalibur™ flow cytometer (BD Biosciences). Data were analyzed using CELLQuest™ Software (BD Biosciences). At least 10,000 cells per sample were analyzed.

2.5. RTD-PCR

RTD-PCR was performed as previously described [12]. Briefly, total RNA obtained from cells using a MicroRNA isolation kit (Stratagene, La Jolla, CA) was reverse-transcribed using 1 μg oligo (dT) primer and Super Script II reverse transcriptase (Invitrogen) in accordance with the manufacturers' protocol. The relative quantities of mRNA expression were analyzed by RTD-PCR using an ABI PRISM 7900 HT Sequence Detection System (Applied Biosystems, Foster City, CA). Primer pairs and probes for BCL-2, BCL-XL, TLR4, MyD88, TNF-α, IL-1β, C/EBP homologous protein (CHOP), immunoglobulin heavy chain binding protein (BiP), CD11b, CD68, and β-actin were obtained from the TaqMan assay reagents library. Gene expression levels were calculated with the $2^{-\Delta\Delta Ct}$ method using β-actin as the internal control.

2.6. TLR ligand stimulation

LPS (1 μg/ml) from *E. coli* (Sigma–Aldrich) was added to conditioned THP-1 cells (3×10^5 cells) or PMA-induced differentiated cells in AIM-V culture medium (Invitrogen). After 3 h incubation, the gene expression of TNF-α and IL-1β was analyzed by RTD-PCR. In addition, the concentration of TNF-α and IL-1β in the culture medium supernatants after 12 h LPS stimulation was measured using an ELISA kit (eBioscience) in accordance with the manufacturer's protocol. With regard to primary human monocytes (5×10^5 cells), the gene expression of TNF-α and IL-1β was analyzed by RTD-PCR after 4 h LPS stimulation. The concentration of TNF-α and IL-1β in the culture medium supernatants after 12 h LPS stimulation was measured using an ELISA kit.

2.7. Measurement of caspase-3 activity

THP-1 cells (3×10^5) were harvested and treated with tunicamycin (5 μg/ml) in RPMI1640 culture medium. After 48 or 72 h incubation, THP-1 cells were lysed, and the DEVD-cleaving activity of active caspase-3 in the lysate was measured using labeled Asp-Glu-Val-Asp-p-nitroanilide (DEVD-pNA) as the substrate and the Caspase-3 Colorimetric Assay Kit (Promega, Madison, WI) in accordance with manufacturer's protocol. The *p*NA light emission was quantified using a microtiter plate reader at a wavelength of 405 nm.

2.8. Western blot

Conditioned THP-1cells were washed twice with PBS and lysed in 100 μl of lysis buffer (10 mM Tris–HCl (pH 7.4), 1% SDS). A total of 10 μg of total proteins were loaded per well and separated on a 7% SDS–PAGE by electrophoresis, followed by transfer to a nitrocellulose membrane. The transferred nitrocellulose membranes were probed with anti-TLR4, anti-MyD88 or anti-β-actin antibody (Cell Signaling Technology, Danvers, MA) at a concentration of 1:500. The secondary goat-anti-rabbit antibody conjugated with horseradish peroxidase (HRP) was used at a concentration of 1:1000 (Cell Signaling Technology). The membrane was visualized by chemiluminescence using the ECL kit (Amersham Biosciences, Piscataway, NJ). Each expression level was assessed and compared to β-actin expression using densitometry.

2.9. Microscopic observation of immunofluorescent cells

For assessment of NF-κB nuclear translocation, THP-1 cells were treated with tunicamycin for 12 h, followed by stimulation with LPS (1 μg/ml) for 40 min. Treated cells were plated at a density of 1×10^5 cells per 22-mm glass coverslip. Cells were fixed for 30 min in cold 4% paraformaldehyde, permeabilized for 2 min at 25 °C in 0.25% Triton X-100 and incubated with PBS supplemented with 10% BSA. Fixed and permeabilized cells were incubated with PBS with 10% BSA containing anti-NF-κB p65 (Cell Signaling Technology). After being washed three times in PBS, coverslips were incubated with the anti-rabbit IgG conjugated with FITC (Jackson Immunoresearch, West Grove, PA). Nuclei were stained with 4, 6-diamino-2-phenylindole (Vector Laboratories, Burlingame, CA). Fluorescent cells were examined with a laser-scanning confocal microscope (Radiance 2100; Bio-Rad, Hercules, CA).

2.10. NF-κB ELISA

Quantitative analysis of NF-κB p65 activation was performed using the CASE™ activation of signaling ELISA kit for NF-κB p65 S536 (SABiosciences Corporation, MD) according to the manufacturer's instructions with slight modifications. Briefly, 1.5×10^4-cells were seeded and incubated on the 96-well plate overnight. Cells were fixed, washed and blocked to avoid non-specific antibody binding. Cells were incubated with anti-pan-NF-κB p65 S536 antibody or anti-phospho-NF-κB specific antibody, washed, and incubated with the secondary antibody. After washing cells, colorimetric detection was performed using a microtiter plate reader at a wavelength of 450 nm.

2.11. Statistical analysis

Data are expressed as means ± SEM. The Mann–Whitney *U* test was applied to assess the significant difference between the two groups. Statistical significance was determined as $P < 0.05$.

3. Results

3.1. Attenuation of TLR signaling prior to apoptosis in human monocytes under ER stress

We examined how ER stress affects the viability of THP-1 cells by assessing the frequency of apoptotic THP-1 cells when treated with tunicamycin (5 μg/ml). Apoptotic cells were defined as cells positive for Annexin-V and negative for 7-AAD by flow cytometry. As shown in Fig. 1A and B, a low frequency of apoptotic cells was observed at 12 h. After 24 h, an increased frequency of apoptosis was observed among THP-1 cells treated with tunicamycin compared to untreated cells. When cells were treated with tunicamycin for 48 h and 72 h, the activity of the pro-apoptotic protease, caspase-3, was significantly increased (Fig. 1C). Furthermore, the expression of the anti-apoptotic genes, BCL-2 and BCL-XL was substantially lower in tunicamycin-treated THP-1 cells compared with untreated cells (Fig. 1D). When cells were treated with tunicamycin, the activity of the pro-apoptotic protease caspase-3 was significantly increased after 48 h (Fig. 1C), though not at 12 h (data not shown). We also observed similar results using 1 μg/ml tunicamycin treatment, but alternations were less compared with 5 μg/ml tunicamycin treatment (data not shown). These results suggest that ER stress induced conventional apoptosis in the human monocytic cell line.

Monocytes typically express pattern-recognition molecules such as TLRs that are important for innate immunity against various pathogens. TLR4 is the receptor for the LPS ligand, and plays a role in host defense against gram-negative infection [13]. To determine whether THP-1 cells were functionally affected under ER stress induced by tunicamycin treatment, we assessed the responsiveness of THP-1 cells to LPS stimulation *in vitro*.

We examined whether the expression of TLR4 and MyD88, a crucial adaptor molecule for TLR signaling, was affected in THP-1 cells under ER stress induced by tunicamycin treatment at 12 h. We confirmed that tunicamycin treatment induced ER stress on THP-1 cells at 12 h, observing that the expression levels of pivotal genes related to ER stress, CHOP and BiP, were up-regulated (Fig. 2A). Whereas expression of TLR4 and MyD88 was not affected

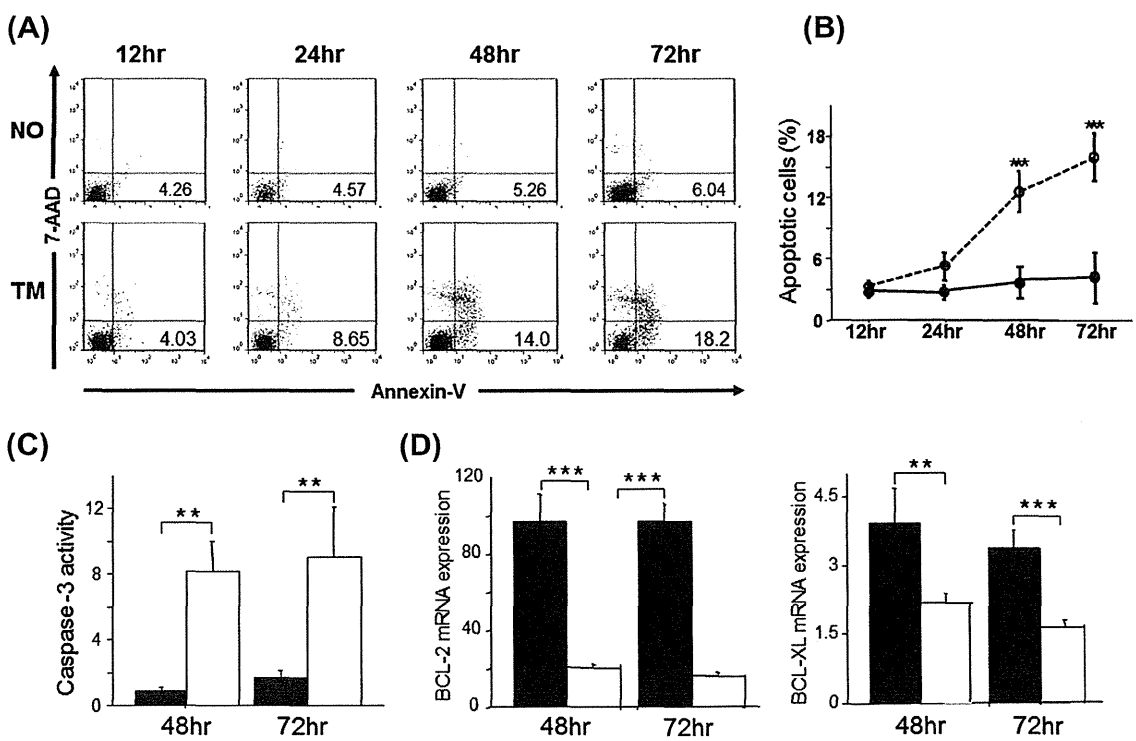

Fig. 1. ER stress increased the susceptibility of THP-1 cells to apoptosis. (A–B) THP-1 cells were incubated in culture medium supplemented with tunicamycin (5 μg/ml). The frequency of apoptotic cells was analyzed by flow cytometry at 12 h, 24 h 48 h and 72 h. More apoptotic cells were observed among the THP-1 cells treated with tunicamycin for more than 48 h incubation compared to the untreated THP-1 cells. (A) A representative scatter gram of Annexin-V and 7-AAD for THP-1 cells treated with tunicamycin. The numbers in each quadrant indicate the percentage of apoptotic cells. (B) The average number of apoptotic cells was calculated in triplicate for each condition. (C) Caspse-3 activity in THP-1 cells treated with tunicamycin was significantly increased at 48 h and 72 h incubation. (D) The BCL-2 and BCL-XL expressions in THP-1 cells incubated with tunicamycin for 48 h and 72 h were significantly down-regulated. Filled circle, no treatment; open circle, treatment with tunicamycin (5 μg/ml). TM, tunicamycin. Data are expressed as means ± SEM. $^{**}P < 0.01$, $^{***}P < 0.001$.

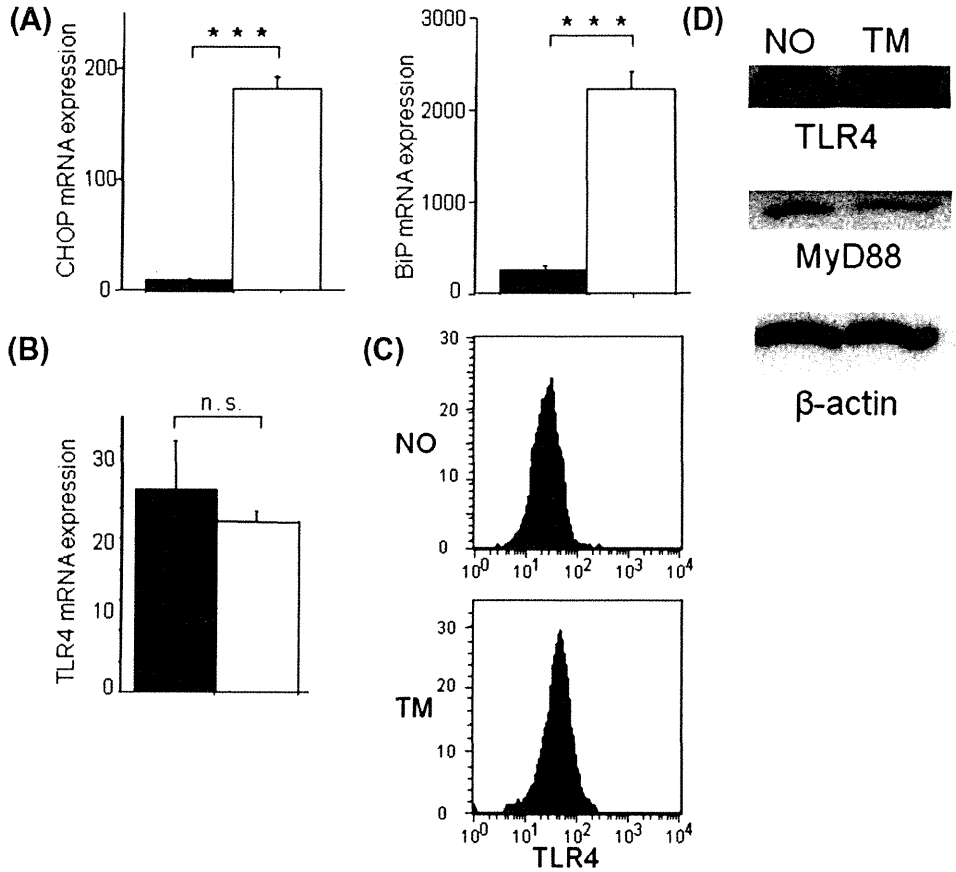

Fig. 2. Tunicamycin treatment induced ER-stress related molecules, but did not affect the expression of TLR4 and its accessory molecule MyD88 in THP-1 cells. (A) The transcriptional expression levels of the ER stress markers CHOP and BiP in THP-1 cells incubated with tunicamycin for 12 h were significantly up-regulated (RTD-PCR). Data are expressed as means ± SD of four independent experiments. (B–C) The expression of TLR4 was not affected by 12 h incubation with tunicamycin, as assessed by RTD-PCR (B), flow cytometry (C) and Western blot (D) Similarly, MyD88 expression was not affected (D). Filled bars, no treatment; open bars, treatment with tunicamycin (5 μg/ml). ***$P < 0.001$.

with 12 h incubation with tunicamycin (Fig. 2B–D), the gene expression of the proinflammatory cytokines, TNF-α and IL-1β, was down-regulated in the tunicamycin-treated THP-1 cells that were stimulated with LPS for 3 h (Fig. 3A). Concomitantly, the concentration of TNF-α and IL-1β in culture medium was also decreased after 12 h stimulation with LPS (Fig. 3B), indicating that the production of these cytokines from THP-1 cells was diminished. We also observed similar results using a lower concentration of tunicamycin (1 μg/ml), along with another ER stress inducer, thapsigargin, which is an endoplasmic reticulum Ca^{2+} ATPase inhibitor (Supplemental Fig. 1). Both 12 h tunicamycin (1 μg/ml) and 12 h thapsigargin (3 μM) treatments induced ER stress, but did not induce apoptosis, alteration of caspase-3 activity, or expression of anti-apoptotic genes (data not shown).Furthermore, we confirmed a similar effect of ER stress attenuation of TLR4 signaling in primary human monocytes (Fig. 3C and D). The gene expression of IL-1β was significantly down-regulated in tunicamycin-treated primary human monocytes that were stimulated with LPS for 4 h (Fig. 3C), and the gene expression of TNF-α was slightly down-regulated. The concentration of TNF-α and IL-1β in culture medium was also decreased after 12 h stimulation with LPS (Fig. 3D). These results demonstrate that TLR signaling in human monocytes under tunicamycin-induced ER stress was functionally impaired with regard to the TLR4 stimulation-signaling to produce proinflammatory cytokines.

3.2. ER stress inhibited the activation of NF-κB in THP-1 cells stimulated with LPS

To further assess how ER stress affects the expression of proinflammatory cytokines, we examined the expression of NF-κB, a pivotal transcriptional factor of proinflammatory cytokines [14,15]. THP-1 cells treated with tunicamycin were stimulated with LPS, and the activation of NF-κB was assessed every 40 min up to 120 min. Before LPS stimulation, no significant difference in NF-κB activation was observed, with or without treatment of tunicamycin in THP-1 cells (Fig. 4A). However, after LPS stimulation, NF-κB activation was not induced in THP-1 cells under ER stress compared with untreated THP-1 cells (Fig. 4A). Concomitantly, the translocation of NF-κB into the nucleus induced by LPS stimulation for 40 min was not observed in untreated THP-1 cells when cells were under ER stress (Fig. 4B). Furthermore, we examined the translocation of NF-κB induced by TNF-α stimulation in THP-1 cells under ER stress to clarify whether other stimulation also affects the activation of NF-κB under ER stress. We did not observed significant translocation of NF-κB following TNF-α stimulation, as compared with LPS stimulation (Supplemental Fig. 2), suggesting that the effect on NF-κB mobilisation under ER stress was caused only by TLR signaling. These results demonstrate that activation of NF-κB in response to the LPS stimulation was impaired in THP-1 cells under ER stress.